



---

**Universidad de Valladolid**

**FACULTAD DE CIENCIAS**

**TRABAJO FIN DE MASTER**

**Máster en Técnicas Avanzadas en Química.  
Análisis y Control de Calidad Químicos**

**Evaluating the Efficiency of Ion Exchange in Sr Isotope Analysis for  
Paleomobility Research**

**Autora: Marta María Gil Fernández**

**Tutor: Fernando Jiménez Barredo**

**Director: Altug Hasözbeq (CENIEH)**

**2024**

# Abbreviations

ICP-MS: Inductively Coupled Plasma Mass Spectrometer

SF-ICP-MS: Sector Field Inductively Coupled Plasma Mass Spectrometer

MC ICP-MS: Multicollector Inductively Coupled Plasma Mass Spectrometer

ICP-OES: Inductively Coupled Plasma Optic Emission Spectrometer

PCA: Principal Components Analysis

FA: Factorial Analysis

HCA: Hierarchical Clustering Analysis

## Acknowledgments

This study has been carried out in the Uranium Series Laboratory, part of the Geochronology Department at the National Centre for Human Evolution Research (CENIEH). The samples and instruments were provided by

I would like to thank my supervisor, Dr. Altug Hasózbek, for patiently guiding me through this master thesis and teaching me about the incredible world of strontium isotope research. I have learned not only in a theoretical perspective, but also in a practical way, understanding how to be a better professional and person.

I would also like to thank my academic supervisor Dr. Fernando Jiménez Barredo for teaching me invaluable lessons about chemistry and the professional practice of this discipline. My perspective has widened and I have improved as a person as a result.

I would like to thank my family for being a rock this whole time. Even though we are geographically apart, their support has never wavered and for that I am extremely grateful.

Thank you to my friends, for all the words of encouragement they have offered me when the stress and fatigue got to me. Each and every one of you are incredible people I'm proud to have by my side.

Finally, I would like to thank Ángela de la Hoz Nieto. You have been a fundamental support in the duration of this whole thesis. Without you, this process would have been definitely more difficult and less enjoyable.

# Index

Resumen .....	4
ABSTRACT .....	5
1. Introduction .....	7
1.1. Isotopes and their applications .....	7
1.2. Strontium Isotopes in Geological and Environmental Studies .....	8
1.3. Strontium isotopes in paleomobility research .....	9
1.4. Extraction techniques for strontium isotope analysis .....	12
2. Objectives .....	13
3. Experimental .....	14
3.1. Samples .....	15
3.1.1. Pre-treatment of Plant samples .....	17
3.3. Analytical Methods .....	19
3.3.2. Clean Lab Analysis (Ion Chromatography) .....	20
3.4. Mass Spectrometry .....	22
3.5. Statistical Analysis .....	25
4. Results and Discussion .....	26
4.1. Elemental analysis: ICP-OES and SF-ICP-MS .....	26
4.2. Isotopic analysis .....	30
4.2.1. Hand-made cartridges .....	33
4.2.2. Commercial cartridges .....	33
4.2.3. Comparison between both cartridges .....	34
4.3. Statistical analysis .....	37
4.3.1. Pearson correlation coefficeints matix .....	38
4.3.2. Principal components analysis (PCA) .....	39
4.3.3. Factorial analysis (FA) .....	42
4.3.4. Classification of samples depending on their origin or nature .....	47
5. Conclusions .....	49
6. References .....	51
Lista de Figuras .....	58
Lista de Tablas .....	60

## Resumen

Este estudio propone un método de trabajo para la preparación de muestras con diferentes matrices destinadas al análisis isotópico y de concentración de estroncio, así como su análisis estadístico. El objetivo es crear un modelo de reconocimiento de patrones para su posterior aplicación en el mapeo de la abundancia isotópica del estroncio en la península ibérica.

Las muestras de plantas y suelos (n=12) se obtuvieron de varias regiones de la península ibérica. Dos métodos cromatográficos se evaluaron para la extracción del estroncio y su posterior análisis en MC ICP-MS: cartuchos de resina hechos a mano y cartuchos de resina comerciales. Los cartuchos hechos a mano exhibieron una mayor precisión, mientras que la extracción con cartuchos comerciales fue más rápida y con resultados comparables. Para las muestras purificadas con cartuchos hechos a mano se obtuvieron rangos de  $^{87}\text{Sr}/^{86}\text{Sr}$  de entre 0.70897-0.70918 para las muestras de arena de cuevas, de 0.70887 para la arena de playa, de 0.70814 para los sedimentos del río Guadiana, de 0.70826 para la tierra de cultivo y de 0.71192 para el material de referencia NIST 8704. Para las muestras botánicas se obtuvo: un valor de entre 0.70904-0.70922 para el trigo de burgos, de 0.70930 para el trigo de Tudela de Navarra y un valor de 0.70971 para el material de referencia NIST 4356. Para las muestras purificadas con cartuchos comerciales se obtuvieron rangos en muestras de suelos de: 0.69071-0.70942 para las arenas de cuevas, de 0.70884 para la arena de playa, de 0.70690 para los sedimentos del río Guadiana, de 0.70816 para la tierra de cultivo, y de 0.70123 para el material de referencia NIST 8704. Para las muestras botánicas se obtuvo: un valor de entre 0.70908-0.70917 para el trigo de burgos, de 0.70931 para el trigo de Tudela de Navarra y un valor de 0.70982 para el material de referencia NIST 4356.

La concentración total de estroncio en las muestras se midió después de una digestión ácida total usando SF-ICP-MS e ICP-OES. Para las muestras de suelo: de arena de cuevas se obtuvo un rango de concentración de 50.21-120.28 mg/Kg, para la muestra de arena de playa un rango entre 449.48-750.97 mg/Kg, para los sedimentos del río Guadiana un valor de 285.18 mg/Kg, para la tierra de cultivo 648.07 mg/Kg y para el material de

referencia NIST 8704 un valor de 129.27 mg/Kg. Para las muestras botánicas: para el tallo del trigo de Burgos se obtuvo un valor de 631.05 mg/Kg, para las cáscaras, semillas y semillas completas de ese mismo trigo se obtuvieron valores de 322.93 mg/Kg, 679.55 mg/Kg, 526.64 mg/Kg, para el trigo de Tudela de Navarra se obtuvo un valor de 613.78 mg/Kg, y para el material de referencia NIST 4356 se obtuvo un valor de 188.41 mg/Kg.

Todas estas variables fueron utilizadas en el análisis estadístico por componentes principales (PCA), análisis factorial (FA) y análisis de agrupamiento jerárquico (HCA). Las muestras demostraron una tendencia a agruparse según su origen y naturaleza. Aunque con limitaciones debido al espacio muestral, se consiguió desarrollar un método de análisis experimental y estadístico para contribuir a la investigación del mapeo isotópico del estroncio en la península ibérica.

## ABSTRACT

This study proposes a frame work for different matrices sample preparation, aimed at isotopic and strontium concentration analysis, as well as the statistical analysis of them. The objective is to create a pattern recognition model for subsequent application in mapping the isotopic abundance of strontium in the Iberian Peninsula (isoscape). Plant and soil samples (n=12) were obtained from various regions of the Iberian Peninsula. Two chromatographic methods were evaluated for the extraction of strontium and its posterior analysis by MC ICP-MS: hand-made resin cartridges and commercial resin cartridges. Hand-made cartridges exhibited higher precision, while extraction with commercial cartridges was faster and with comparable results to the hand-made cartridges ones. For samples purified with handmade resin cartridges,  $^{87}\text{Sr}/^{86}\text{Sr}$  ranges were 0.70897-0.70918 for cave sand samples, 0.70887 for beach sand, 0.70814 for Guadiana River sediments, 0.70826 for crop soil, and 0.71192 for NIST 8704 reference

material. For botanical samples, values obtained were: 0.70904-0.70922 for Burgos wheat, 0.70930 for Tudela de Navarra wheat, and 0.70971 for NIST 4356 reference material. For results of commercial cartridges the values for soil samples were of 0.69071-0.70942 for cave sand samples, 0.70884 for beach sand, 0.70690 for Guadiana River sediments, 0.70816 for crop soil, and 0.70123 for NIST 8704 reference material. For botanical samples, values obtained were: 0.70908-0.70917 for Burgos wheat, 0.70931 for Tudela de Navarra wheat, and 0.70982 for NIST 4356 reference material.

Strontium concentration in the samples was measured after total acid digestion, using SF-ICP-MS and ICP-OES. For soil samples: cave sand concentration values ranged from 50.21-120.28 mg/kg, beach sand values ranged between 449.48-750.97 mg/kg, The concentration of Guadiana River sediments was 285.18 mg/kg, crop soil's was 648.07 mg/kg, and NIST 8704 reference material had a value of 129.27 mg/kg. For botanical samples: Burgos wheat stem measured at 631.05 mg/kg, while chaffs, seeds, and whole seeds of the same wheat measured 322.93 mg/kg, 679.55 mg/kg, and 526.64 mg/kg, respectively. Tudela de Navarra wheat yielded 613.78 mg/kg, and NIST 4356 reference material measured 188.41 mg/kg.

All these variables were used for the statistical analysis, using principal component analysis (PCA), factor analysis (FA) and hierarchical clustering analysis (HCA). All samples showed a tendency to cluster with similar natured ones, as well as with similar origin ones. Despite limitations due to sample size, the experimental and statistical work frame was successfully developed to contribute to the investigation of strontium isotopic mapping in the Iberian Peninsula.

Keywords: strontium isoscape,  $^{87}\text{Sr}/^{86}\text{Sr}$  ratio, MC-ICP-MS, ICP-MS, ICP-OES, statistical analysis, Strontium isotopic mapping, Iberian Peninsula, strontium resin cartridges

# 1. Introduction

Strontium (Sr) isotopic analysis has become an invaluable tool for paleomobility research, offering insight into the movement patterns and origin of ancient humans and animal populations [1, 2, 3, 4]. This research uses Sr isotopes a form of tracking the mobility of said groups and their geographical origin, since the Sr isotopic signature for each region will be different [5, 6]. Sampling and analytical techniques are key for the accuracy and precision of Sr isotope ratios, since the latter ones are directly dependent on the techniques used [7, 8]. This small study aims to evaluate the efficiency of two different chromatography procedures (hand-made and commercial resin cartridges) for Sr analysis in various matrices, including standard materials, soils, sediments and biological samples. It aims, as well, to develop a robust and precise work frame for unequivocally distinguish between the origins of samples and speed up these kinds of analysis.

For the purpose of this study, samples (n=12) were screened for Sr concentrations using two techniques: Sector-Field Inductively Coupled Plasma Mass Spectrometry (SF-ICP-MS) and Inductively Coupled Plasma Optical Emission Spectroscopy (ICP-OES). For Sr isotopic ratios, two types of resin cartridges were tested for ion chromatography on their effectiveness and to extract the Sr from diverse matrices and to accurately determine their respective Sr ratio.

This thesis is constructed on the basis of developing a fast and accurate sample preparation procedure for paleomobility studies. In the first segment there is a comparison between two different ion chromatography techniques, to evaluate the difference between their Sr isotopic ratios and to accurately determine their Sr concentration. The second segment covers the statistical approach of this study, assessing the influence of said variables on their origin classification.

By conducting this research, this study aims to provide a fast and reliable procedure for Sr isotopic analysis, enhancing the accuracy of isotopic data and thereby improving our understanding of paleomobility patterns where applicable.

## 1.1. Isotopes and their applications

Isotopes, following IUPAC definition [9], are “Nuclides having the same atomic number but different mass numbers.” Each element has different number of isotopes

and relative abundances in the environment, with its exact values being recorded in digital resources as well as in physical ones.

The unique characteristics of each element's isotope, as well as their interactions with the environment, make them an essential research tool in valuable fields such as geology, medicine, archaeology, forensic sciences, chemistry or restoration. [4, 10].

Radiogenic and non-radiogenic isotopes have different applications depending on their stability. From Uranium Series dating to environmental studies involving carbon, nitrogen, oxygen and hydrogen isotopes; the versatility of isotopes' study is widely recognized [11, 12, 13, 14]. In more recent times, it was the recent technological advances which have enhanced their utility in many fields [15, 16]. Particularly in earth sciences, where they provide insights into geochemical processes such as ore deposits, thermodynamic changes, contamination and dating [15, 16, 17, 18]. The accuracy of these techniques has made isotopic analysis essential in geological studies, with dating methods such as U-Pb, Sm-Nd or Rb-Sr being prominent based on their mineral type [19, 20].

## 1.2. Strontium Isotopes in Geological and Environmental Studies

Among isotopes, strontium isotopes are especially significant due to their wide spread of applications in studies such as geology and environmental studies [21, 22].

Strontium is a soft alkaline metal, with a  $Z=38$  and an atomic standardized weight of  $82.62 \pm 0.01$  g/mol [23, 24]. It is commonly found in two ores Strontianite ( $\text{SrCO}_3$ ) and Celestine ( $\text{SrSO}_4$ ), as well as in mica group minerals [25]. Strontium ionic radius (1.18 Å) is very similar to that of calcium (0.99 Å), and their chemical properties are quite similar [26, 27, 28]. This similarity allows strontium to replace calcium in the crystalline lattice of many minerals [18, 19]. Strontium has four naturally occurring isotopes:  $^{84}\text{Sr}$  (0.56%),  $^{86}\text{Sr}$  (9.86%),  $^{87}\text{Sr}$  (7.00%) and  $^{88}\text{Sr}$  (82.58%) [25, 26, 29]. Only  $^{87}\text{Sr}$  is radiogenic, meaning it is the product of the radioactive decay chain of  $^{87}\text{Rb}$  [30]. It is also used in geological dating, since it accumulates in potassium rich minerals [31, 32, 33, 34] and, therefore, allows for the determination of their age.

The  $^{87}\text{Sr}/^{86}\text{Sr}$  ratio is particularly valuable in geochronology due to the stable baseline provided by  $^{86}\text{Sr}$ , enabling the detection of changes in  $^{87}\text{Sr}$  abundance. It is used in dating marine sediments; organisms incorporate Sr isotopes into their shells, preserving the isotopic signature of the seawater at that time [35, 36, 37]. This provides valuable information on continental weathering processes and environmental changes [17, 26, 38, 39, 40]. Strontium isotopes are affected by weathering of the country rock, and it depends on how old is that rock and its composition. The resulting strontium from weathering transfers to the soil, sediment, tree and plant. Once this products are consumed by mammals (animals and humans), Sr transfers to the skeleton of the bodies (**Figure 1**).

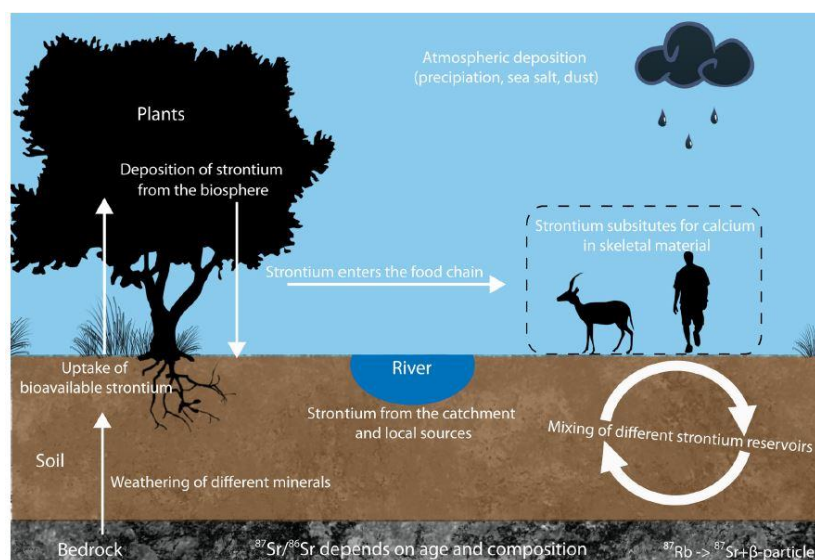


**Figure 1.** Strontium cycle and its influences. [41]

### 1.3. Strontium isotopes in paleomobility research

Studies of provenance and paleomobility are another interesting branch of strontium isotope research. Strontium can substitute calcium in hydroxyapatite ( $\text{Ca}_5(\text{PO}_4)_3$ ) in bones and teeth, preserving the geological fingerprint and allowing to trace its origin [30, 31]. However, bones or teeth are not closed systems and can undergo diagenetic processes that alter the expected isotopic ratios. This requires a correction for mass dependent fractionation, traditionally applied as  $\delta^{88}\text{Sr}/^{86}\text{Sr}$  directly to the data obtained by analytical techniques such as ICP-MS (**Equation 1**) [42, 43, 44].

$$\delta^{88}\text{Sr}/^{86}\text{Sr} (\text{‰}) = [({}^{88}\text{Sr}/^{86}\text{Sr})_{\text{sample}} / ({}^{88}\text{Sr}/^{86}\text{Sr})_{\text{SRM987}} - 1] \times 1000 \quad (\text{Equation 1})$$

Mapping isotopic abundance in a certain region, known as creating an isoscape [45, 46], has become an essential tool in provenance studies. These maps, constructed from extensive sampling and statistical analysis, provide spatial predictions of isotopic values, proving useful for rapid and accurate sample provenance determination. These isoscapes are very valuable in archaeology, since they allow for migratory analysis of ancient populations, while minimizing the sampling needed for each research. Therefore, isoscapes it reduces the research costs and improve data accuracy.

Globally, there has been a general analysis of mean values of isotope ratios in different matrices (**Figure 2**).

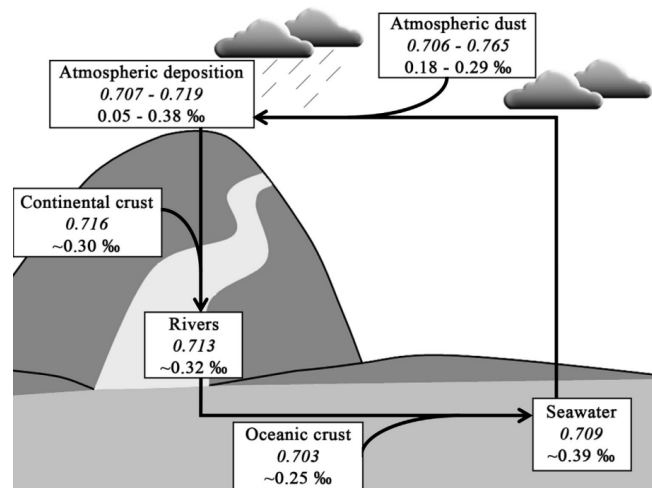


**Figure 2.** Range of variation of  $^{87}\text{Sr}/^{86}\text{Sr}$  ratios (values in italic) and  $\delta^{88}\text{Sr}/^{86}\text{Sr}$  (‰) values in rocks, atmospheric dust and different water compartments at global scale [3].

Depending on the lithology of the samples, different Sr values vary (**Table 1**).

**Table 1.** Strontium concentration on different nature samples [41].

Nature	Material	Sr (mg/Kg)
Geological	Sandstone	20
	Low-Ca granite	100
	Deep-sea clay	180

**Table 1** (continuation). Strontium concentration on different nature samples [41].

Nature	Material	Sr (mg/Kg)
Geological	Syenite	200
	Shale	300
	High Ca-granite	440
	Ultramafic rock	1
	Basalt	500
	Deep-sea carbonate	2000
	Carbonate	600
Soils	Soil minerals	10-1000
	Labile soil minerals	0.2-20
	Soil moisture	0.001-0.07
Water	Seawater	8
	Rivers	0.006-0.8
	Rain	0.001-4
	Snow	0.00001-0.001
Biological	Edible Plants	1-100
	Mammal bone	100-1000+
	Mammal enamel	50-500+

Geologic samples exhibit significant variations in strontium (Sr) concentrations (**Table 1**) [41]. For instance, sandstone contains 20 mg/Kg Sr, while high-Ca granite has 440 mg/Kg Sr.

Soil samples also show a wide range of Sr concentrations, reflecting the heterogeneous nature of soil composition; for example, soil minerals can contain Sr from 10 to 1000 mg/Kg, whereas labile soil minerals have lower Sr levels (0.2 to 20 mg/Kg). In aquatic environments, seawater typically has 8 mg/Kg Sr, while river water shows lower Sr (0.006 to 0.8 mg/Kg) levels.

Biological materials, such as edible plants and mammal bones, provide insight into the bioavailability and incorporation of Sr, with plants containing 1 to 100 mg/Kg Sr, and bones having 100 to 1000+ mg/Kg Sr. These variations are essential for understanding

geochemical processes, nutrient cycling, and tracing the movement and diet of ancient populations.

Additionally, a couple of studies have already been performed in Europe, with different degrees of depth [46, 47, 48, 49, 50, 51]. Since the samples used on this study have their origin in Spain, the focus is the studies performed in Portugal [52, 53] and Spain [54].

#### 1.4.Extraction techniques for strontium isotope analysis

For a precise Sr isotope analysis, the separation of said element from the matrix is an indispensable step [55]. It is usually performed using ion exchange chromatography; its accuracy is crucial for the analysis. This study evaluates the usage of two different types of resin cartridges (hand-made and commercial) for the separation of Sr from standard materials, soils, sediments and organic samples. They were analysed for Sr concentrations using SF-ICP-MS and ICP-OES, and the isotopes ratio was measured using MC ICP-MS [56].

The separation process begins with a digestion or leaching of samples, depending if the aim is to measure concentration or isotope ratios [57, 58]. In biological samples, additional steps such as ashing or H<sub>2</sub>O<sub>2</sub> addition are necessary to remove organic matter [59]. Either technique is followed by ion chromatography to purify the Sr, using a special Sr resin. While total acid digestion ensures complete Sr availability, leaching offers a simpler alternative for certain soil types since it concentrates the Sr and allows for a more intense signal in the instrument [60, 61].

This research aims to optimize the Sr-separation processes to build a robust sample preparation protocol for paleomobility studies. By improving the precision of Sr isotope analysis, we can enhance our understanding of ancient human and animal movements, contributing valuable data to archaeological and geological research.

## 2. Objectives

The objective of this master's thesis is to develop a robust chemical and statistical methodology for constructing a comprehensive  $^{87}\text{Sr}/^{86}\text{Sr}$  ratio map (isoscape) of Spain, thereby contributing to the field of paleo-mobility research.

To achieve this, the study will:

- Evaluate the precision and reliability of two ion chromatography resin cartridges for strontium separation (hand-made and commercial), analyzing geological samples with different matrixes.
- Develop an efficient and systematic procedure for mapping different geographical regions using a large number of samples.
- Establish a sophisticated statistical framework to classify samples based on their geographical origin. This method will not only consider the  $^{87}\text{Sr}/^{86}\text{Sr}$  ratio but also account for strontium concentration variations, enhancing the ability to discriminate between similar sites and providing a more detailed understanding of the origin's isotopic profile.

### 3. Experimental

This study aimed to develop a robust work frame for sample preparation intended for isotopic analysis, evaluating the efficacy of different chromatography methods for Sr extraction in samples with different matrices. Its impact on Sr concentration and Sr isotope ratios was also tested.

Samples of soil and plants (n=12) were collected from diverse geographical locations across the Iberian Peninsula. Prior to Sr analysis, the samples underwent rigorous preparation, including acid digestion and leaching, specific to the sample type. Subsequently, Sr was extracted using two chromatography methods—handmade and commercial resin cartridges. Analytical measurements were performed using ICP-OES and SF-ICP-MS for Sr concentrations and MC ICP-MS for isotope ratios.

Once the experimental part was performed, statistical analyses, including PCA, HCA, and FA, were conducted to correlate the results with geographical locations and test the reliability of the extraction methods (Figure 3).

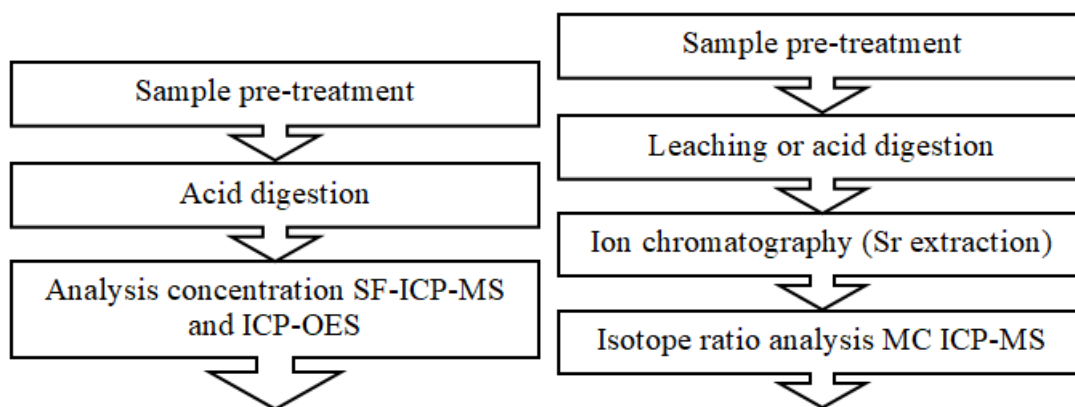


**Figure 3.** Work flow of the steps followed in the laboratory work. The one on the left is the work flow for isotopic analysis, and the one on the right is the one for concentration analysis.

The details of the methodology, analytical techniques and instrumentation are summarized below.

### 3.1. Samples

In this study, a variety of samples were analyzed to test different Sr extraction techniques and determine their Sr concentrations and isotope ratios. Samples were provided by CENIEH department of Geochronology. Two types of samples were analyzed: soil and plants (**Table 2**). To compare their values to the Sr isoscape of the Iberian Peninsula, soil samples were collected from various geographical locations (Figure 4). Wheat was selected as the cereal plant for this study.

**Table 2.** Summary of the samples used in this study

Type	Sample	Nature	Origin
Biological	Wheat	Whole plant	Burgos, Spain
	Wheat	Seeds	Tudela, Spain
Soil	LM-21154-01	Cave sand	Gibraltar
	LM-21154-02	Cave sand	Gibraltar
	LM-21154-04	Cave sand	Gibraltar
	KARRASPIO	Beach sand	Karraspio, Spain
	LM-21312-01	Fluvial Sediment	Guadiana River
	TIERRAN	Wheat crop soil	Tudela, Navarra, Spain



**Figure 4.** Map of Iberian Peninsula Spain. The red circles indicate the origins of the samples.

Grains of wheat were collected from Burgos, Spain, and dried at 60°C (**Figure 5**).



**Figure 5.** Grains of wheat taken from Burgos (Spain)

Bare wheat seeds were sourced from Tudela, Navara, Spain (Figure 6), with their red color indicating a common fungicide treatment.

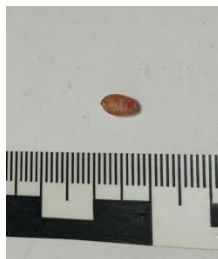


**Figure 6.** Wheat seeds from Tudela (Navarra, Spain)

Soil samples (Figure 7) varied visually and were collected from depths to avoid surface soil variability. Table 3 summarizes the sample characteristics, and Figure 4 provides a geographical summary of the sample origins.

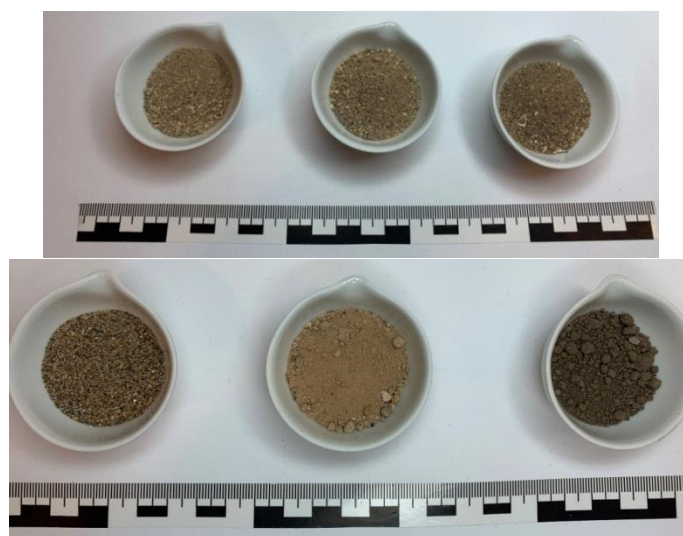


**Figure 7.** Soil samples. From left to right, top to bottom: LM 21154-01, LM21154-02, LM21154-04, KARRASPIO, LM21312-01, TIERRAN.

*Specific sample locations used in this thesis are:*

**Karraspio Beach Sand:** Chosen for its proximity to the prehistoric site of Ekain (Guipuzkoa), where CENIEH has conducted studies.

**Tudela Soil and Wheat Samples:** Selected due to their proximity to archaeological sites in La Rioja, Aragón, and Navarre.

**Burgos Wheat:** Chosen for its proximity to the Atapuerca site, enabling the study of both regional soil and organic matter.

**Guadiana River Sediments:** Selected due to numerous archaeological sites along its course.

**Gibraltar Cave Sands:** Chosen for their proximity to significant prehistoric cave sites.

*Reference Materials used in this thesis are:*

NIST SRM8704: Buffalo river sediment with a standardized Sr value of 126.19-141 mg/Kg, used for soil samples.

NIST SRM4356: Ashed bone with a standardized Sr value of 173 mg/Kg, used for plant samples.

NIST SRM987: Powdered SrCO<sub>3</sub>, used for <sup>87</sup>Sr/<sup>86</sup>Sr ratio analysis (**Table 3**).

**Table 3.** Expected values of <sup>87</sup>Sr/<sup>86</sup>Sr ratio for SRM987

Reference Material	<sup>88</sup> Sr/ <sup>86</sup> Sr	<sup>87</sup> Sr/ <sup>86</sup> Sr	<sup>84</sup> Sr/ <sup>86</sup> Sr
NIST SRM 987	8.37861 ± 0.00325	0.71034 ± 0.00026	0.05655 ± 0.00014

### 3.1.1. Pre-treatment of Plant samples

Plant samples require pre-treatment before strontium separation. For wheat, four types of samples were collected: stems, seeds with chaff, bare seeds, and chaff alone. The stem was cut into 2 cm sections (**Figure 8**) and halved lengthwise and horizontally.

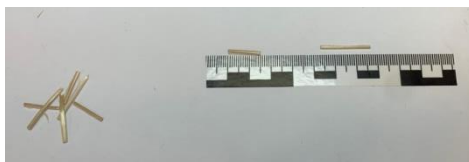


**Figure 8.** Cut up sections of the wheat stem.

Chaff was separated from the whole seed (**Figure 9**), and the resulting material was ground in a NAHITA 70 mL agate mortar until homogeneous, then stored in Eppendorf tubes for further experiments. The agate mortar was rinsed between samples with water and isopropanol to prevent contamination.



**Figure 9.** From left to right, whole seed, bare seeds and chaffs.

### 3.2. Lab Materials

*The lab materials used for this study included the following items:*

NAHITA 70 mL agate mortar, VWR 25 mL porcelain evaporating dish (crucible), PFA 10 mL vials, Mettler Toledo Delta Range Analytical balance with 0.00001 g resolution Endecott sieve (1 mm), Acid-resistant chromatography columns

*The reagents used were the following:*

Ultrapure double distilled HNO<sub>3</sub> (15 M) and HCl (12 M), Acetic acid glacial for analysis, ACS, ISO, MilliQ Type I water with 18.2 Ω·cm @ 25°C purity, Strontium standards for calibration with a nominal concentration of 1000 µg·g<sup>-1</sup> in 2% HNO<sub>3</sub>.

*Resins used for extraction chemistry:*

Sr-Resin® (4,4'(5')-di-t-butylcyclohexano 18-crown-6 in octane, with particle size 50-100 µm) from Eichrom Technologies.

A Thermo Scientific Thermolyne oven was used for ashing samples at the required temperatures (**Figure 10**).



**Figure 10.** Oven at CENIEH laboratory

Acid digestion was performed using an ultraWave Single Reaction Chamber microwave digestion system (Milestone connect) (**Figure 11**), capable of reaching up to 300°C and 199 bar pressure, allowing different matrices and acid mixtures within a single reaction vessel.



**Figure 11.** ultraWave Single reaction chamber microwave digestion at CENIEH laboratory

### 3.3. Analytical Methods

#### 3.3.1. Acid Digestion and Leaching

The procedure is adapted from a Portugal isoscape study [52]. Samples were ashed at 450°C for at least 12 hours for biological sample acid digestion. A subsample of 10 mg

was digested with 2 mL of 7 N HNO<sub>3</sub> at 140°C for 48 hours using a microwave digester. The solution was transferred to containers, evaporated at 90°C, and re-dissolved in 5 mL of 3 M HNO<sub>3</sub>.

Soil samples were ashed at 450°C for at least 12 hours, sieved through a 1 mm sieve, and the <1 mm fraction was used. A 100 mg subsample was leached with 4 mL of 1 M acetic acid for 30 minutes, sonicated for 15 minutes, and centrifuged. The supernatant was evaporated and re-dissolved in 1 mL of 7 M HNO<sub>3</sub>, then evaporated and re-dissolved in 5 mL of 3 M HNO<sub>3</sub>.

Complete digestion was performed with HF and HNO<sub>3</sub>, for sandy samples including 1 mL of H<sub>2</sub>O<sub>2</sub> to remove biological matter. For Karraspio beach sand, 8 mL of HF was used for complete dissolution.

### 3.3.2. Clean Lab Analysis (Ion Chromatography)

Sr extraction was performed in the ultra-clean lab facilities at CENIEH using two chromatography techniques:

#### *Handmade Cartridge:*

75 µL of Sr-Resin® was loaded into microcolumns (**Figure 12**), conditioned with 3 M HNO<sub>3</sub>, and loaded with 1 mL of sample. The Ca, K, Rb, and Ba fractions were eluted with 3 M HNO<sub>3</sub> and discarded. The Sr fraction was eluted with MQ water, evaporated, and re-dissolved for isotope analysis. The resin was cleaned with 6 M HCl for reuse.

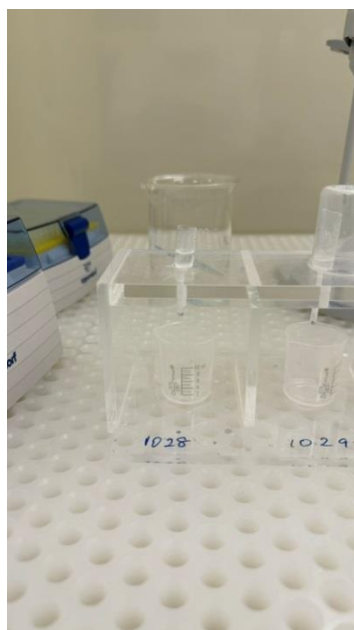


**Figure 12.** Close up of micro column.

*Commercial Cartridges:*

Pre-prepared Sr resin columns from Eichrom® (**Figure 13**) were conditioned with 3 M  $\text{HNO}_3$ , and 1 mL of sample was loaded. Elution followed the same procedure as the handmade cartridge method, with Sr eluted in 0.01 M  $\text{HNO}_3$ .



**Figure 13.** General setup of commercial columns

### 3.4. Mass Spectrometry

Sr concentration analysis was performed using an ICP-OES 5300DV (Perkin Elmer) (Figure 14) and a SF-ICP-MS Element XR (Thermo Scientific) (Figure 15) for validation. Dilutions of 1 mL of sample in 10 mL of 2% HNO<sub>3</sub> were prepared for analysis.

**ICP-OES** is a technique in which the sample is atomized by the plasma, causing an emission of light at characteristic wavelengths depending on the element. This type of analysis technique does not require vacuum and can operate at ambient pressure.

**SF-ICP-MS** is a technique widely utilized in modern chemistry. The magnetic and electric field applied to the ionized atoms allows to separate the atoms depending on their m/z ratio, and to discern the composition of a sample. It can be coupled with other techniques, such as HPLC or laser ablation. This instrument operates at high vacuum and has a high accuracy on the data provided.

Strontium isotope ratios were analyzed using a **Multi-Collector ICP-MS** Neptune (Thermo Scientific) (Figure 16). MC-ICP-MS is an invaluable instrument used for isotopic analysis in the field of geochronology. It is composed by the fusion between a TIMS (thermal ionization mass spectrometer) and a modern mass spectrometer, this coupled with its high resistors allows for its exceptional sensitivity and accuracy. This instrument operates at high vacuum.

The configurations and parameters of all three of the instruments are detailed in **Tables 4, 5, and 6**.



**Figure 14.** ICP-OES at CENIEH.

**Table 4.** Measure parameters of ICP-OES

Measure parameter of ICP-OES

Monitored Wavelengths	407.771 nm 421.552 nm 232.235 nm
Integration mode	Peak area, automatized between 1 and 5, 3
Detection type	Axial
RF (W)	1300
Plasma Gas	15 L · min <sup>-1</sup>
Nebulizer Gas	Ar, 0.8 L · min <sup>-1</sup>
Auxiliary gas	0.2 L · min <sup>-1</sup>
Plasma cut gas	N <sub>2</sub>
Sample gas	1.5 ml·min <sup>-1</sup>
Spray Chamber	Cyclonic gas chamber
Nebulizator	Cross flow
Acquisition software	Syngyxtix
Baseline correction	2 points



**Figure 15.** HR-ICP-MS, ELEMENT XR at CENIEH.

**Table 5.** Measure parameters of HR-ICP-MS, ELEMENT XR.

Measure parameters for ELEMENT, HR-ICP-MS

Acquisition time	5 blocks, 5 cycles (8 mins of each sample)	
First Vacuum	1.22 x 10 <sup>-3</sup> mbar	
High Vacuum	1.41 x 10 <sup>-3</sup> mbar	
RF (W)	1250	
Cooling Gas	16.14 L · min <sup>-1</sup>	
Plasma Gas	0.73 L · min <sup>-1</sup>	
Sample gas	1.211 L · min <sup>-1</sup>	
Spray chamber	PC <sup>3</sup>	
Nebulizator	ST-4907	
Cones	Ni – Skimmer (H49730)	Ni – Sampler (Ni24385)



**Figure 16.** MC-ICP-MS, NEPTUNE at CENIEH.

**Table 6.** Measure parameters of MC-ICP-MS, NEPTUNE.

Measure parameter of MC-ICP-MS, NEPTUNE, Low resolution

RF (W)	1220					
Cooling Gas	15.0 L/min					
Plasma Gas	0.70-0.72 L/min					
Sample gas	0.70-0.75 L/min					
Spray chamber	Concentric PFA 100 $\mu$ L/min					
Desolvation membrane	Aridus II					
Cones	Skimmer Ni (X), Sampler Ni (Jet)					
Faraday cup detectors configuration	<b>L4</b>	<b>L3</b>	<b>L2</b>	<b>L1</b>	<b>C</b>	<b>H1</b>
	$^{83}\text{Kr}$	$^{84}\text{Sr}$	$^{85}\text{Rb}$	$^{86}\text{Sr}$	$^{87}\text{Sr}$	$^{88}\text{Sr}$

### 3.5. Statistical Analysis

Three multivariate analyses were performed: Principal Component Analysis (PCA), Hierarchical Conglomerate Analysis (HCA), and Factorial Analysis (FA) using STATGRAPHICS 19. For HCA, four variables were used: total Sr concentration,

$^{87}\text{Sr}/^{86}\text{Sr}$ ,  $^{88}\text{Sr}/^{86}\text{Sr}$ , and  $^{84}\text{Sr}/^{86}\text{Sr}$ . PCA and FA were standardized, with FA using varimax rotation to identify underlying relations between variables.

## 4. Results and Discussion

### 4.1. Elemental analysis: ICP-OES and SF-ICP-MS

Elemental strontium concentration in samples was determined using ICP-OES, with a cross flow nebulizer due to the presence of insoluble fluorides, and SF-ICP-MS with a PC<sup>3</sup>.

Soil samples show significant variability in strontium concentration (**Table 7**), ranging from 52.21 mg/Kg to 120.28 mg/Kg. Although cave sand samples originate from the same geographical location, their concentration results oscillate considerably: a difference of up to 20 mg/Kg can be seen between LM 21154 samples. The beach sand sample exhibits the highest strontium concentration among all samples (**Table 8**) with a value of 750.97 mg/Kg in the SF-ICP-MS and 449.48 mg/Kg on the ICP-OES. The crop soil sample strontium concentration has a value of 648.07 mg/kg in SF-ICP-MS and 370.54 mg/Kg in ICP-OES (**Table 7**). River sediments, including a reference material employed in this study, exhibit intermediate strontium concentrations, with values of 285.18 mg/Kg and 234.40 mg/Kg in SF-ICP-MS and ICP-OES respectively.

Among plant samples, most values are relatively consistent, with some exceptions such as Wheat Chaff. This is reflected on its concentration, standing at between 322.93 mg/Kg by SF-ICP-MS and 336.41 mg/Kg by ICP-OES for wheat chaff, compared to the concentration between 679.55 mg/Kg by SF-ICP-MS and 682.68 mg/Kg by ICP-OES of wheat bare seeds and of 631.05 mg/Kg by SF-ICP-MS and 658.81 mg/Kg by ICP-OES of wheat stems. Hence, the lower value of 526.64 mg/Kg for the mixture of bare seeds and chaffs.

Elemental Sr analysis of soil leachate samples was conducted, yielding varying results (**Table 9**). However, these values were not usable due to experimental discrepancies

with the Sr concentration in reference material NIST 8704, the approximately five times lower than expected, with a value of 23.37 mg/Kg by ICP-OES and 25.88 mg/kg by SF-ICP-MS (**Table 9**) against the value of 126.19-141 mg/kg recorded in the literature.

For the plant samples there was no leachate, only the product of the acid digestion carried out. Thus, no comparison between concentrations could be made.

Cave sand experience a high variability between results. This can be explained due to differences in carbonate particle distribution within the cave sand, influencing the final strontium concentration results. The sampling method is quite important, yielding different results depending on the varying mineralization of the cave (especially if there is calcite) [62, 63].

Likewise, beach sand has varying concentrations depending on the technique used. This can be due to the proximity of the beach to the ocean. Seawater has a value of approximately 8 mg/Kg (**Table 1**), the constant tide of the ocean can deposit strontium on the beach sand, driving up its overall concentration [15, 64].

Crop soil variability can be due to the use of fertilizers or weathering, since it is from a site used for agriculture for a long time.

For biological samples, the low value of wheat chaffs can be attributed to its fibrous composition, which limits strontium incorporation. Unlike wheat seeds, chaff is more exposed to environmental conditions, enhancing the potential for strontium leaching. Wheat seeds have nutrient-rich biological matter, making the uptake of Strontium easier. The high concentration of wheat stem can be due to it acting as the path for water and nutrients from the soil to the seeds and the rest of the plant [65].

From a general standpoint, concentration results are in accordance with literature on the topic (**Table 1**). No specific research on Sr concentrations on these samples have been made in Spain, which leaves the option to correlate these results with the geological context of those sites.

**Table 7.** Total digestion Sr concentration results in ICP-OES and SF-ICP-MS

Sample	Nature	Origin	Literature values (mg/Kg)	ICP-OES		SF-ICP-MS	
				Sr (mg · Kg <sup>-1</sup> )	σ	Sr (mg · Kg <sup>-1</sup> )	σ
LM 21154-01	Cave Sand	Gibraltar	10-1000	90.20	± 1.1	120.28	± 0.03
LM 21154-02	Cave Sand	Gibraltar		70.70	± 0.4	72.88	± 0.04
LM 21154-04	Cave Sand	Gibraltar		50.68	± 0.8	52.21	± 0.01
KARRASPIO	Beach sand	Karraspio		449.48	± 0.5	750.97	± 0.02
LM 21312-01	River Sediment	Guadiana River		234.40	± 0.5	285.18	± 0.04
TIERRAN	Crop Soil	Tudela	10-1000	370.54	± 1.0	648.07	± 0.04
NIST8704	River Sediment	Buffalo River	126.19-141	120.93	± 1.2	129.27	± 0.07
M.O-1	Wheat stem	Burgos	100	658.81	± 0.7	631.05	± 0.03
M.O-2	Wheat chaff	Burgos		336.41	± 1.8	322.93	± 0.02
M.O-3	Wheat bare seed	Burgos		682.68	± 1.9	679.55	± 0.10
M.O-4	Wheat whole seed	Burgos		534.37	± 1.0	526.64	± 0.01
TRIGON	Wheat bare seed	Tudela		649.36	± 0.3	613.78	± 0.03
NIST 4356	Ashed bone	Unknown	173	191.72	± 0.7	188.41	± 0.03

**Table 9.** Sr leachate concentration results in ICP-OES and SF-ICP-M

Sample	Nature	Origin	Literature values (mg/Kg)	ICP-OES		SF-ICP-MS	
				Sr (mg · Kg <sup>-1</sup> )	σ	Sr (mg · Kg <sup>-1</sup> )	σ
LM 21154-01	Cave Sand	Gibraltar	10-1000	57.15	± 0.75	93.05	± 0.22
LM 21154-02	Cave Sand	Gibraltar		90.44	± 0.42	68.81	± 0.24
LM 21154-04	Cave Sand	Gibraltar		10.60	± 0.71	47.38	± 0.12
KARRASPIO	Beach sand	Karraspio		553.96	± 0.33	523.87	± 0.40
LM 21312-01	River Sediment	Guadiana River		181.45	± 0.63	235.76	± 0.22
TIERRAN	Crop Soil	Tudela	10-1000	386.16	± 0.79	353.55	0.19
NIST8704	River Sediment	Buffalo River	126.19-141	23.37	± 0.94	25.88	± 1.48

#### 4.2. Isotopic analysis

The MC ICP-MS NEPTUNE was first calibrated using the SRM 987 reference material. Its  $^{87}\text{Sr}/^{86}\text{Sr}$  ratio was measured, with values seen in **Table 7** and **9** (since two batches were analysed).

**Table 10.**  $^{87}\text{Sr}/^{86}\text{Sr}$  ratio results for SRM 987.

	First batch	Second batch
$^{87}\text{Sr}/^{86}\text{Sr}$ mean???	$0.71029 \pm 0.000030$	$0.71026 \pm 0.000189$
n	4	3

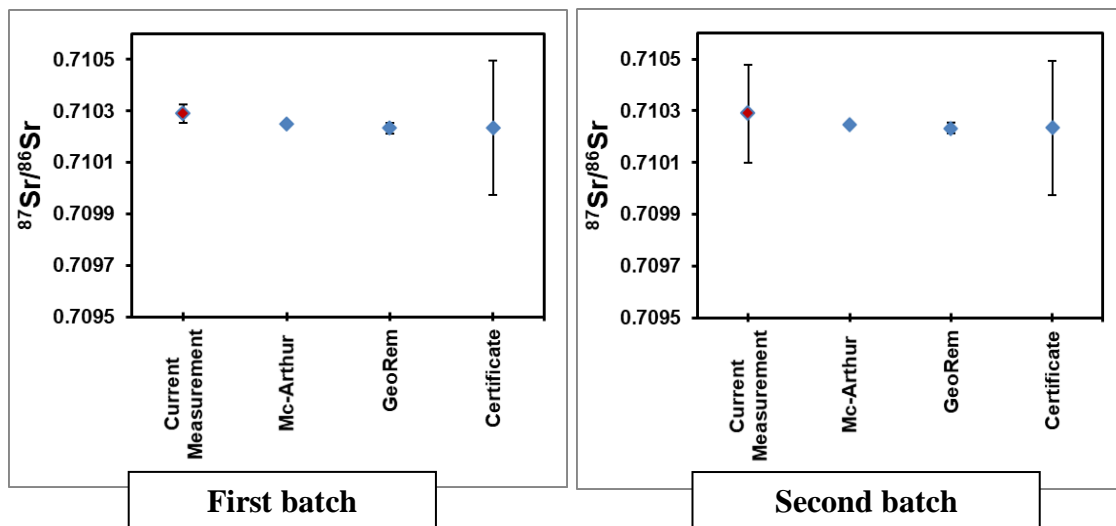


**Figure 17.** Graphical representation of the SRM987  $^{87}\text{Sr}/^{86}\text{Sr}$  ratio experimental measurements along with the literature values.

The experimental value of the SRM987  $^{87}\text{Sr}/^{86}\text{Sr}$  ratio is slightly higher than the literature values (**Figure 17**). Both measurements are quite similar, differing only in the 5th decimal place; however, the error is much higher in the second batch. They fall within the certified possible range, thereby validating the subsequent sample measurements with only very small mass-dependent fractionation changes

**Table 11.**  $^{88}\text{Sr}/^{86}\text{Sr}$  and  $^{84}\text{Sr}/^{86}\text{Sr}$  ratios of the samples

Sample	Nature	Origin	MC ICP-MS handmade cartridge		MC ICP-MS commercial cartridge	
			$^{87}\text{Sr}/^{86}\text{Sr}$	$\sigma$ ( $\times 10^{-4}$ )	$^{87}\text{Sr}/^{86}\text{Sr}$	$\sigma$ ( $\times 10^{-4}$ )
LM 21154-01	Cave Sand	Gibraltar	0.70918	$\pm 2.17$	0.70942	$\pm 7.60$
LM 21154-02	Cave Sand	Gibraltar	0.70917	$\pm 0.96$	0.70801	$\pm 4.28$
LM 21154-04	Cave Sand	Gibraltar	0.70897	$\pm 2.65$	0.69071	$\pm 43.93$
KARRASPIO	Beach sand	Karraspio	0.70887	$\pm 0.34$	0.70884	$\pm 1.30$
LM 21312-01	River Sediment	Guadiana River	0.70814	$\pm 1.13$	0.70690	$\pm 3.12$
TIERRAN	Crop Soil	Tudela	0.70826	$\pm 0.74$	0.70816	$\pm 0.91$
NIST8704	River Sediment	Buffalo River	0.71192	132.46	0.70123	$\pm 11.12$
M.O-1	Wheat stem	Burgos	0.70904	$\pm 0.28$	0.70908	$\pm 0.40$
M.O-2	Wheat chaff	Burgos	0.70922	$\pm 0.85$	-	-
M.O-3	Wheat bare seed	Burgos	0.70912	$\pm 0.35$	0.70913	$\pm 0.46$
M.O-4	Wheat whole seed	Burgos	0.70916	$\pm 0.16$	0.70917	$\pm 0.99$
TRIGON	Wheat bare seed	Tudela	0.70930	$\pm 0.41$	0.70931	$\pm 0.58$
NIST 4356	Ashed bone	Unknown	0.70971	$\pm 3.21$	0.70982	$\pm 0.33$

**Table 12.**  $^{88}\text{Sr}/^{86}\text{Sr}$  and  $^{84}\text{Sr}/^{86}\text{Sr}$  ratios for samples

Sample	Nature	Origin	MC ICP-MS home-made cartridge		MC ICP-MS commercial cartridge		MC ICP-MS home-made cartridge		MC ICP-MS commercial cartridge	
			$^{88}\text{Sr}/^{86}\text{Sr}$	$\sigma$ ( $\times 10^{-3}$ )	$^{88}\text{Sr}/^{86}\text{Sr}$	$\sigma$ ( $\times 10^{-4}$ )	$^{84}\text{Sr}/^{86}\text{Sr}$	$\sigma$ ( $\times 10^{-4}$ )	$^{84}\text{Sr}/^{86}\text{Sr}$	$\sigma$ ( $\times 10^{-4}$ )
LM 21154-01	Cave Sand	Gibraltar	8.37982	$\pm 2.85$	8.39699	$\pm 100.77$	0.05700	$\pm 0.52$	0.05951	$\pm 51.37$
LM 21154-02	Cave Sand	Gibraltar	8.37859	$\pm 0.96$	8.39288	$\pm 66.74$	0.05698	$\pm 0.34$	0.05721	$\pm 10.44$
LM 21154-04	Cave Sand	Gibraltar	8.38255	$\pm 4.17$	8.18187	$\pm 349.32$	0.05888	$\pm 2.27$	0.12715	$\pm 110.93$
KARRASPIO	Beach sand	Gipuzkoa	8.38145	$\pm 0.88$	8.39238	$\pm 10.45$	0.05652	$\pm 0.05$	0.05659	$\pm 1.99$
LM 21312-01	River Sediment	Guadiana River	8.38393	$\pm 1.05$	8.38872	$\pm 56.01$	0.05673	$\pm 0.27$	0.05766	$\pm 16.99$
TIERRAN	Crop Soil	Tudela	8.38614	$\pm 1.52$	8.39059	$\pm 17.59$	0.05647	$\pm 0.12$	0.05680	$\pm 4.73$
NIST8704	River Sediment	Buffalo River	8.45105	$\pm 126.98$	8.28412	$\pm 268.81$	0.06635	$\pm 57.46$	0.08982	$\pm 46.21$
M.O-1	Wheat stem	Burgos	8.38876	$\pm 1.19$	0.05648	$\pm 7.24$	0.05608	$\pm 0.21$	0.05648	$\pm 0.14$
M.O-2	Wheat chaff	Burgos	8.38613	$\pm 0.34$	-	-	0.05640	$\pm 0.02$	-	-
M.O-3	Wheat bare seed	Burgos	8.38370	$\pm 1.48$	0.05637	$\pm 7.56$	0.05632	$\pm 0.15$	0.05637	$\pm 0.59$
M.O-4	Wheat whole seed	Burgos	8.39172	$\pm 0.70$	0.05638	$\pm 6.22$	0.05645	$\pm 0.04$	0.05638	$\pm 0.81$
TRIGON	Wheat bare seed	Tudela	8.38751	$\pm 3.48$	0.05644	$\pm 15.18$	0.05644	$\pm 1.36$	0.05644	$\pm 0.37$
NIST 4356	Ashed bone	Unknown	8.38637	$\pm 1.08$	0.05663	$\pm 11.45$	0.05643	$\pm 0.10$	0.05663	$\pm 1.28$

#### 4.2.1. Hand-made cartridges

For soil samples the values have a slight variation (**Table 11**). In cave sands the values range from 0.70918 to 0.70897. Between the three values is that of LM 21154-04 that has the biggest difference with the same nature samples, with a value of 0.70897 compared to the values of 0.70918 and 0.70917 of LM 21154-01 and LM 21154-02 respectively. The beach sand sample, KARRASPIO, stands at 0.70887.

Guadiana river sediments, LM 21314-01, have a value of 0.70814. The difference between these river sediments and the Buffalo River sediments (reference material NIST 8704) is high, with the latter one having a value of 0.71192. This is, however, the sample with the highest error amongst the hand-made cartridges samples, and the value could change once the appropriate corrections have been made. For the crop soil the  $^{87}\text{Sr}/^{86}\text{Sr}$  ratio has a value of 0.70826.

In plant samples of wheat from Burgos, the  $^{87}\text{Sr}/^{86}\text{Sr}$  ratios vary in the range 0.70904-0.70922 (**Table 11**). Wheat stem stand with the value of 0.70904 n/n, the lowest of all the values. For bare seeds this value falls in the middle of the range, with 0.70912, and similar to that of whole seeds, with 0.70916. Chaffs have the highest isotope ratio, with 0.70922. The  $^{87}\text{Sr}/^{86}\text{Sr}$  ratio of Navarre's wheat is the highest among wheat samples, with 0.70930. This variation can be due to the different  $^{87}\text{Sr}/^{86}\text{Sr}$  ratio across the plant, due to the slight changes suffered in the trophic chain. However, it's the reference material NIST 4356 which has the highest value, with 0.70971.

#### 4.2.2. Commercial cartridges

The values obtained with commercial cartridges for cave sand samples, LM 21154,  $^{87}\text{Sr}/^{86}\text{Sr}$  ratio differ slightly from each other (**Table 11**). LM 21154-01 and LM 21154-02 are slightly more similar between each other, with 0.70942 and 0.70801, comparing to the value of LM 21154-04 with 0.69071.

For the beach sand sample, KARRASPIO, the value is 0.70884. Crop soil from Navarra has a value of 0.70123. Guadiana river sediments sample has a value of 0.70690, whereas the Buffalo river sediment (reference material NIST 8704) has a value of 0.70123. This gives a slight indicator of its different geological precedence, since both rivers have a very different lithology, reflected in their distinct  $^{87}\text{Sr}/^{86}\text{Sr}$  ratios.

The values for plant samples of wheat from Burgos range from 0.70908 to 0.70917 (**Table 11**). Only the stem (0.70908), bare seed (0.70913) and whole seed (0.70917) was analysed, demonstrating a high similarity between each other. The wheat from Navarra, TRIGON, stands at 0.70931, slightly higher than the highest value from Burgos wheat. The ashed bone, reference material NIST 4356, possess the highest value of  $^{87}\text{Sr}/^{86}\text{Sr}$  ratio, with 0.70982.

#### 4.2.3. Comparison between both cartridges

The comparison between values obtained using hand-made cartridges and commercial ones demonstrate a strong similarity (**Figure 18, 19, 20, 21**). The most differentiated values are the cave sands (LM 21154) samples, as well as the Guadiana river sediments (LM 21314-01). In samples LM 21154-04 and TIERRAN the error is extremely high compared to the rest of the samples, and coincidentally also correspond with the samples with the most variation in the  $^{87}\text{Sr}/^{86}\text{Sr}$  value. This can be due to a system fail in the uptake of the data, which can be corrected afterwards.

Within each sample, the graphical variation is minimal (**Figure 18, 19, 20, 21**). Between different samples a small variation can be seen, due to the difference in decimals depending on their origin.

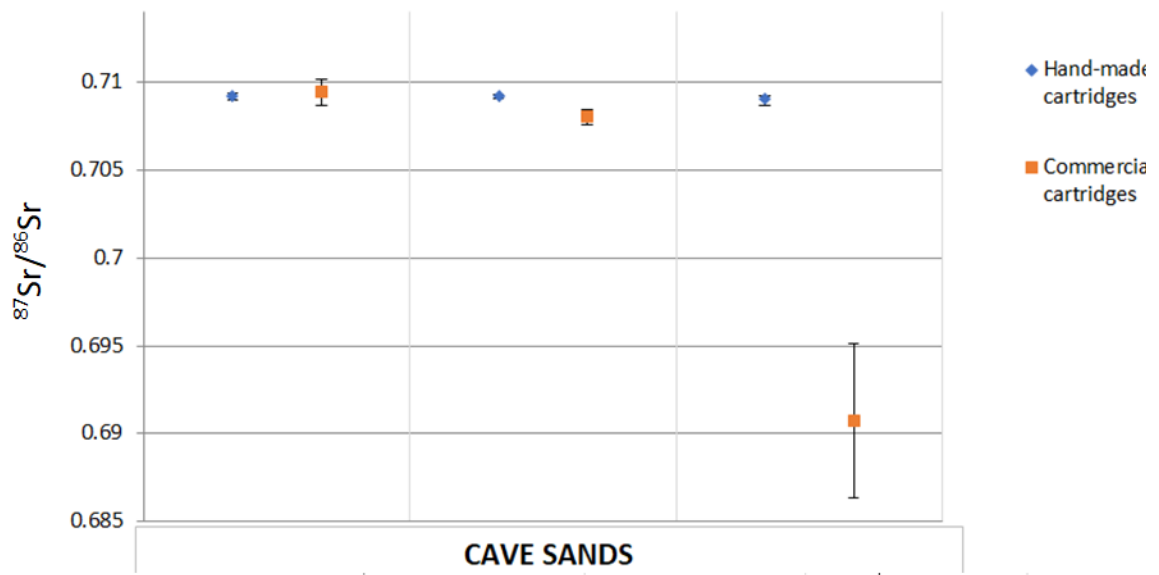


**Figure 18.** Comparison between cave sands'  $^{87}\text{Sr}/^{86}\text{Sr}$  ratios from hand-made and commercial cartridges for the samples (From left to right, each pair of dots: LM 21154-01, LM21154-02, LM 21154-04)

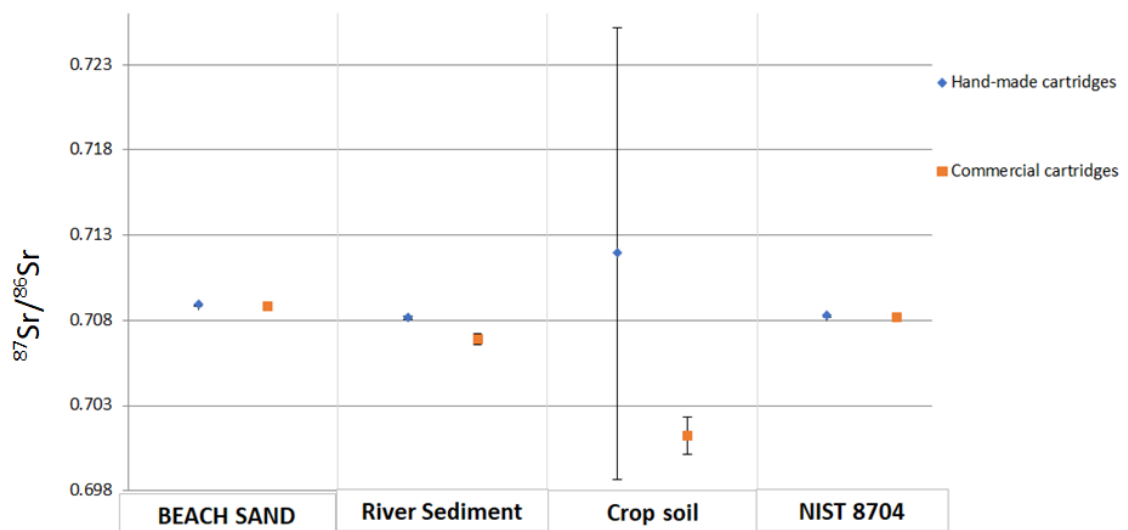


**Figure 19.** Comparison between beach sand, river sediment, crop soil and NIST 8704  $^{87}\text{Sr}/^{86}\text{Sr}$  ratios from hand-made and commercial cartridges for the samples (From left to right, each pair of dots: KARRASPIO, LM 21314-01, TIERRAN, NIST 8704)



**Figure 20.** Comparison between Burgos wheat  $^{87}\text{Sr}/^{86}\text{Sr}$  ratios from hand-made and commercial cartridges for the samples (From left to right, each pair of dots: M.O.-1, M.O.-2, M.O.-3, M.O.-4)

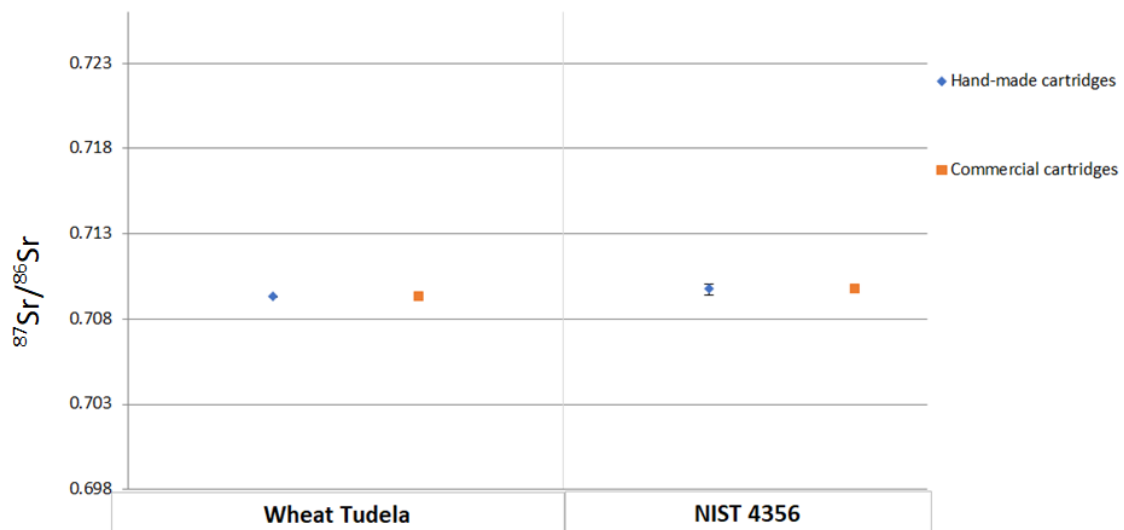


**Figure 21.** Comparison between Tudela wheat and NIST 4356  $^{87}\text{Sr}/^{86}\text{Sr}$  ratios from hand-made and commercial cartridges for the samples (From left to right, each pair of dots: TRIGON, NIST 4356)

### 4.3. Statistical analysis

This study aims to not only propose a sample preparation adequate for isotopic analysis, but also to provide an adequate statistical work frame that allows for every variable to be taken into account when classifying samples.

Firstly, a preliminary general multivariant analysis will be performed, with the objective of discerning the importance of the Pearson correlation coefficient matrix between variables. A distribution univariant analysis will be carried as well, using the Kolmogorov-Smirnov test to assess how the distribution of each variable is.

A principal component analysis (PCA) will be performed, to find the most influential variables. A factorial analysis (FA) will be performed as well, coupled with a hierarchical cluster analysis (HCA) on similarity basis.

Some tendencies in samples have already been appreciated in the results, such as the correlation between concentration and  $^{87}\text{Sr}/^{86}\text{Sr}$  ratios. However, to assess whether these variations are significant or part of the experimental work, a statistical analysis has been performed.

A Kolmogorov-Smirnov test was performed before proceeding with the rest of the analysis to assess the distribution of each set of samples, in case they followed a normal distribution with a 95% confidence interval.

As the hypothesis for this test we will have:

H<sub>0</sub>: The variable follows a normal distribution with 95% of confidence interval.

H<sub>1</sub>: The variable does not follow a normal distribution with 95% of confidence interval.

Only the elemental Sr follows an apparent normal distribution, since its p-value is higher than 0.05 (**Table 13**). The rest of the variables (isotopic ratios) do not surpass the 0.05 threshold value and therefore, the H<sub>0</sub> can be rejected. The  $^{87}\text{Sr}/^{86}\text{Sr}$ ,  $^{88}\text{Sr}/^{86}\text{Sr}$  and  $^{84}\text{Sr}/^{86}\text{Sr}$  variables do not follow a normal distribution (**Table 13**).

**Table 13.** KS test resulting values for each variable

	DMAS	DMINUS	DN	p-value
Sr	0.170	0.166	0.170	0.375
$^{87}\text{Sr}/^{86}\text{Sr}$	0.294	0.363	0.363	0.001
$^{84}\text{Sr}/^{86}\text{Sr}$	0.334	0.361	0.361	0.001
$^{88}\text{Sr}/^{86}\text{Sr}$	0.381	0.354	0.381	0.000

4.3.1. Pearson correlation coefficients matrix

In this case (**Figure 22**) the  $^{87}\text{Sr}/^{86}\text{Sr}$  ratio and  $^{88}\text{Sr}/^{86}\text{Sr}$  ratio are the most strongly correlated, with a positive value of 0.95. The  $^{87}\text{Sr}/^{86}\text{Sr}$  and  $^{84}\text{Sr}/^{86}\text{Sr}$  ratios also exhibit a strong correlation, but it is inversely proportional with a value of -0.75. The strontium concentration is somewhat related to the  $^{87}\text{Sr}/^{86}\text{Sr}$ , with a value of 0.09. The correlation between the  $^{88}\text{Sr}/^{86}\text{Sr}$  and  $^{84}\text{Sr}/^{86}\text{Sr}$  ratios is -0.55, indicating an inverse proportional relationship, similar to the correlation between the  $^{84}\text{Sr}/^{86}\text{Sr}$  and strontium concentration.

The critical r value of the sample matrix is 0.301, for the matrix analysed. Therefore we can apply this value as a threshold for the Pearson correlation coefficients matrix of the different variables.

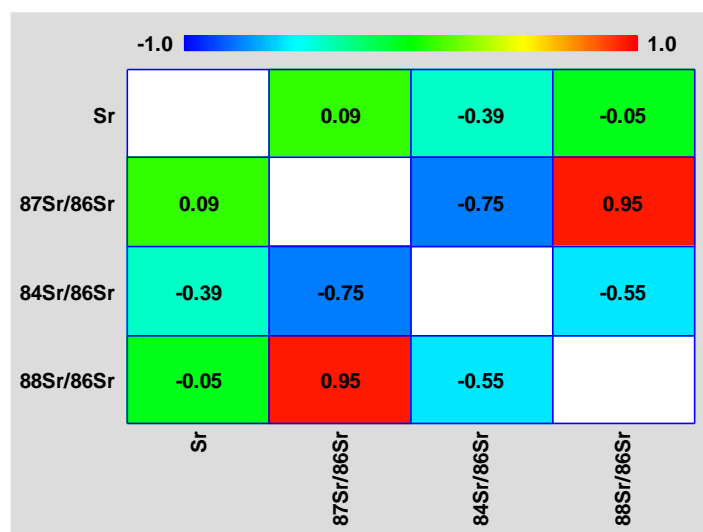


**Figure 22.** Pearson correlation coefficients matrix for the different variables.

Although the correlation matrix contains all the values between each variable, it must be noted that only those with a p-value under 0.05 are statistically significant. Only the correlations between Sr and  $^{84}\text{Sr}/^{86}\text{Sr}$ ,  $^{84}\text{Sr}/^{86}\text{Sr}$  and  $^{87}\text{Sr}/^{86}\text{Sr}$ ,  $^{87}\text{Sr}/^{86}\text{Sr}$  and  $^{88}\text{Sr}/^{86}\text{Sr}$ , and  $^{84}\text{Sr}/^{86}\text{Sr}$  and  $^{88}\text{Sr}/^{86}\text{Sr}$  are statistically significant, according to their p-values (**Table 14**).

**Table 14.** P-values for the correlation matrix.

	Sr	$^{87}\text{Sr}/^{86}\text{Sr}$	$^{84}\text{Sr}/^{86}\text{Sr}$	$^{88}\text{Sr}/^{86}\text{Sr}$
Sr		0.626	0.038	0.787
$^{87}\text{Sr}/^{86}\text{Sr}$	0.626		0.000	0.000
$^{84}\text{Sr}/^{86}\text{Sr}$	0.038	0.000		0.00
$^{88}\text{Sr}/^{86}\text{Sr}$	0.787	0.000	0.000	

#### 4.3.2. Principal components analysis (PCA)

PCA is performed to reduce the dimensions of the data matrix while preserving the most information. In this case, it is set to a listwise method with the limit value for the eigenvalue being 1. The resulting values can be seen in **Table 15**. As shown, the variation can be explained using only PC1 and PC2, which together explain 91.92% of the variation.

It is interesting to look at the eigenvalue: a value greater than 1 indicates how much that single variable can explain. The higher the eigenvalue, the more significance that variable holds. In this case, only two eigenvalues are greater than 1; PC1 and PC2 (**Table 15**). Therefore, those will be the components used to explain the 91.924 % of the variable (**Figure 23**).

**Table 15.** Values for the principal components.

	PC1	PC2	PC3	PC4
Eigenvalue	2.550	1.126	0.310	0.012
Variation	63.754	28.170	7.763	0.313
Percentage				
Accumulated percentage	63.754	91.924	99.687	100.000

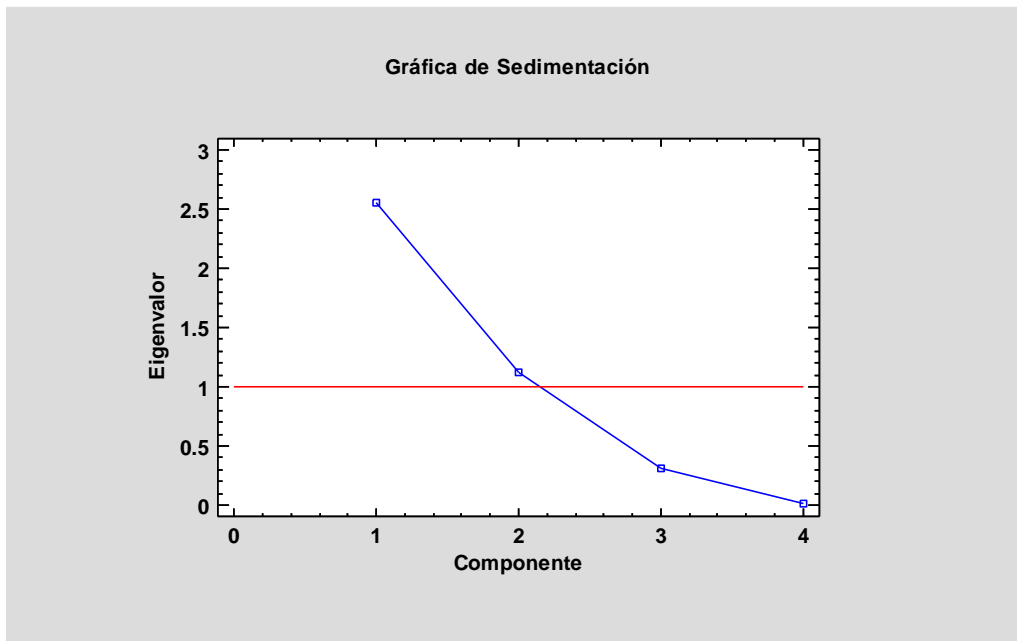


**Figure 23.** PCA sedimentation graph.

After this initial approach, the 4-component matrix is reduced to a 2-component matrix, with values for each variable (**Table 16**). These values will be used to calculate the principal components for the samples.

**Table 16.** Weight of each component for the variables.

	PC1	PC2
Sr	0.152	0.884
$^{87}\text{Sr}/^{86}\text{Sr}$	0.613	-0.160
$^{84}\text{Sr}/^{86}\text{Sr}$	-0.535	-0.284
$^{88}\text{Sr}/^{86}\text{Sr}$	0.560	-0.335

Using these values the resulting loading values for each sample are calculated (**Table 17**).

**Table 17.** Loadings of principal components.

Sample	Nature	PC1	PC2
H-LM 21154-01	cave sand	0.036	-0.705
H-LM 21154-02	cave sand	0.001	-0.833
H-LM 21154-04	cave sand	-0.073	-0.943
C-LM 21154-01	cave sand	0.125	-0.853
C-LM 21154-02	cave sand	0.181	-0.929
C-LM 21154-04	cave sand	-6.894	-0.591
H-KARRASPIO	beach sand	0.334	1.109
C-KARRASPIO	beach sand	0.424	1.051
H-LM21314-01	river sediment	0.014	-0.244
C-LM21314-01	river sediment	-0.002	-0.282
H-NIST 8704	river sediment	0.690	-1.335
C-NIST 8704	river sediment	-3.118	-0.544
H-TIERRAN	crop soil	0.243	0.813
C-TIERRAN	crop soil	0.256	0.787
C-M.O.-1	wheat B	0.333	0.743
C-M.O.-3	wheat B	0.281	0.934
C-M.O.-4	wheat B	0.249	0.473
C-TRIGON	wheat T	0.333	0.702
H-M.O.-1	wheat B	0.380	0.730
H-M.O.-2	wheat B	0.218	-0.149
H-M.O.-3	wheat B	0.361	0.888
H-M.O.-4	wheat B	0.357	0.405
H-TRIGON	wheat T	0.382	0.671
C-NIST 4356	ashed bone	0.195	-0.540
H-NIST 4356	ashed bone	0.221	-0.552
HC-SRM 987	SRM 987	0.680	1.754
C-SRM 987	SRM 987	0.632	1.780
Soil-BLK	blk	3.356	-2.984
Biological-BLK	blk	-0.196	-1.360

There is a slight tendency on numbers at first sight. However, a factorial analysis must be performed to understand the contribution of each factor towards the variables.

#### 4.3.3. Factorial analysis (FA)

For Factor Analysis (FA), the aim is not to reduce the matrix while conserving the most information possible, but to identify hidden correlations between the variables.

##### Without rotation

The two first factors explain approximately 91.92% of the variance (**Table 18**). The  $^{84}\text{Sr}/^{86}\text{Sr}$  isotopic ratio exhibits an inverse trend than the other variables: it starts with a negative value and slowly progresses into higher positive values (**Table 18**).

**Table 18.** Loadings of FA without rotation.

	Factor 1	Factor 2	Factor 3	Factor 4	Communality
Sr	0.243	0.938	0.246	-0.001	1.000
$^{87}\text{Sr}/^{86}\text{Sr}$	0.979	-0.170	0.068	0.086	1.000
$^{84}\text{Sr}/^{86}\text{Sr}$	-0.855	-0.301	0.421	0.028	1.000
$^{88}\text{Sr}/^{86}\text{Sr}$	0.895	-0.356	0.261	-0.067	1.000
Eigenvalue	2.550	1.127	0.310	0.0125	4.000
% Variation	63.754	28.17	7.763	0.313	100

The scores are calculated from the product of these loadings' matrix and the samples matrix. Since the two first factors explain approximately 92% of the variance, only those will be selected for the scores calculation. . The first factor has coefficients more closely related to isotopic relations; therefore it will be called "isotopic profile" (**Table 19**). Meanwhile, the second factor is strongly related to the elemental Sr.

**Table 19.** Scores of each one of the samples.

Sample	Score 1	Score 2
H-cave sand	0.058	-0.749
H-cave sand	0.002	-0.885
H-cave sand	-0.116	-1.001
C-cave sand	0.199	-0.905
C-cave sand	0.290	-0.986
C-cave sand	-11.009	-0.627
H-beach sand	0.533	1.177
C-beach sand	0.676	1.116

**Table 19 (Continuation).** Scores of each one of the samples.

Sample	Score 1	Score 2
H-river sediment	0.022	-0.259
C-river sediment	-0.003	-0.299
H-river sediment	1.102	-1.417
C-river sediment	-4.980	-0.577
H-crop soil	0.389	0.863
C-crop soil	0.409	0.836
C-wheat B	0.532	0.789
C-wheat B	0.449	0.992
C-wheat B	0.398	0.502
C-wheat T	0.532	0.745
H-wheat B	0.607	0.775
H-wheat B	0.349	-0.158
H-wheat B	0.577	0.943
H-wheat B	0.570	0.430
H-wheat T	0.610	0.713
C-ashed bone	0.311	-0.573
H-ashed bone	0.353	-0.586
HC-SRM 987	1.086	1.862
C-SRM 987	1.009	1.890
blk	5.359	-3.167
blk	-0.313	-1.444

From this table, a couple of tendencies can be observed. For Score 1, which is related to isotopic fingerprint, samples that show higher correlation with it include the wheat samples, the beach sand sample, and the SRM987 material, indicating highly similar isotopic fingerprints among them. Low values on Score 1, observed mostly in the soil samples, suggest less similarity in isotopic fingerprint and composition.

For Score 2, which relates to strontium concentration, it can be compared with the concentration values obtained in **Table 7**. Following this reference, higher values on Score 2 indicate lower strontium concentration in the sample. This is why blank samples have the highest score, whereas beach sand samples or wheat samples have negative scores, despite having the highest overall concentration.

Throughout the scores, a clear tendency towards clustering based on the nature of samples can be observed. For example, cave sands exhibit similar score values among them, but they differ significantly from the scores of wheat samples.

This can be further confirmed when looking at the 2D dispersion graph (**Figure 24**): there can be seen at least two differentiated groups when representing Factor 1 vs Factor 2.

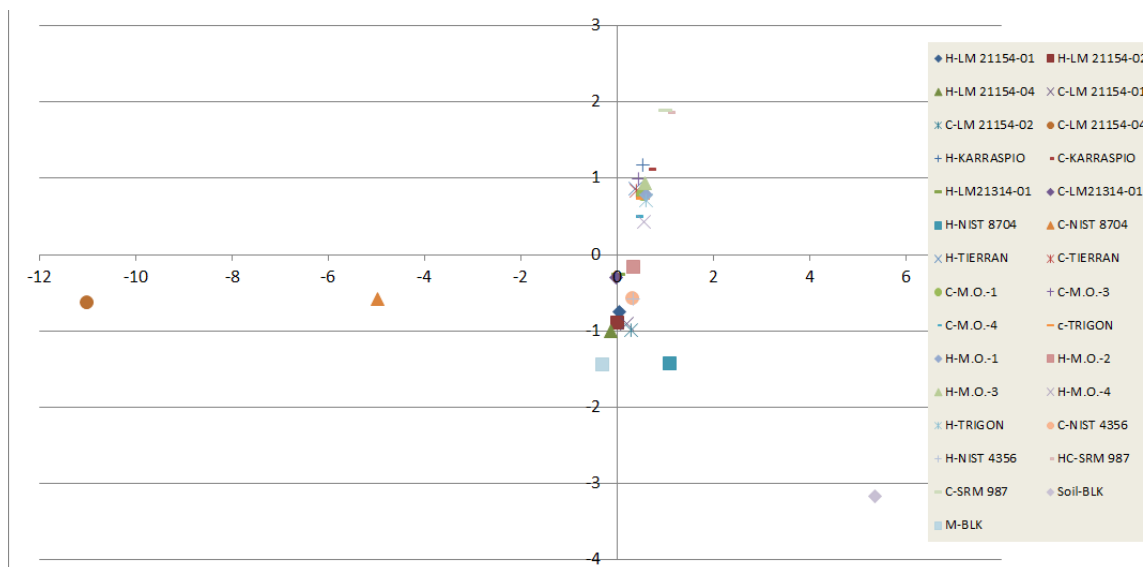


**Figure 24.** Dispersion graph between Factor 1 and Factor 2.

With Varimax rotation

This analysis aims to maximize the primary correlation for each variable while minimizing other relationships to achieve a clearer understanding of the analysis.

In this case, the tables of the contributing factors are slightly different. Whereas in the FA without rotation the loadings matrix before rotating and after rotating was identical, in this case it differs quite a bit (**Table 20 and 22**).

**Table 20.** Loadings before rotating

	Factor 1	Factor 2	Factor 3	Factor 4	Communality
Sr	0.243	0.938	0.246	0.243	1.000
<sup>87</sup> Sr/ <sup>86</sup> Sr	0.979	-0.170	0.068	0.979	1.000
<sup>84</sup> Sr/ <sup>86</sup> Sr	-0.855	-0.301	0.421	-0.855	1.000
<sup>88</sup> Sr/ <sup>86</sup> Sr	0.895	-0.356	0.261	0.895	1.000

**Table 20 (continuation).** Loadings before rotating

	Factor 1	Factor 2	Factor 3	Factor 4	Communality
Variation	2.550	1.127	0.311	0.013	4.000
% Variation	63.754	28.170	7.763	0.313	100.000

**Table 21.** Loadings after varimax rotation.

	Factor 1	Factor 2	Factor 3	Factor 4	Communality
Sr	-0.029	-0.173	0.984	0.003	1.00
<sup>87</sup> Sr/ <sup>86</sup> Sr	0.888	-0.446	0.043	0.101	1.00
<sup>84</sup> Sr/ <sup>86</sup> Sr	-0.393	0.885	-0.248	-0.001	1.00
<sup>88</sup> Sr/ <sup>86</sup> Sr	0.975	-0.206	-0.061	-0.059	1.00

After obtaining these values, the scores for the samples are obtained (**Table 22**) following the same procedure as without the rotation.

**Table 22.** Scores for the samples with Varimax rotation

Nature of sample	Score 1	Score 2
H-cave sand	-0.293	-0.781
H-cave sand	-0.332	-0.847
H-cave sand	-0.255	-0.674
C-cave sand	0.019	-0.426
C-cave sand	-0.101	-0.719
C-cave sand	-2.498	3.921
H-beach sand	-0.036	-0.089
C-beach sand	0.097	-0.021
H-river sediment	-0.291	-0.656
C-river sediment	-0.221	-0.545
H-river sediment	1.157	0.692
C-river sediment	-1.272	1.484
H-crop soil	-0.090	-0.220
C-crop soil	-0.036	-0.167
C-wheat B	-0.031	-0.207
C-wheat B	-0.129	-0.214
C-wheat B	-0.141	-0.368
C-wheat T	-0.052	-0.236
H-wheat B	0.004	-0.223
H-wheat B	-0.139	-0.563
H-wheat B	-0.020	-0.168
H-wheat B	0.017	-0.288

**Table 22 (Continuation).** Scores for the samples with Varimax rotation

Nature of sample	Score 1	Score 2
H-wheat T	0.019	-0.203
C-ashed bone	-0.175	-0.690
H-ashed bone	-0.145	-0.693
HC-SRM 987	0.260	0.290
C-SRM 987	0.198	0.266
blk	4.255	2.171
blk	0.231	0.172

It validates the observed pattern in the unrotated data. In this instance, comparing Factor 1 with Factor 3 (which exhibits a relatively consistent value across all samples) yields **Figure 25**. The data demonstrates a distinct association of the first factor with the samples' geographical origin, evident from their clustering. Given the strong correlation of Score 1 with isotopic fingerprint, we can assert that isotopic ratios are pivotal for categorizing samples based on their origin, underscoring their significance as a powerful statistical tool for large-scale studies.

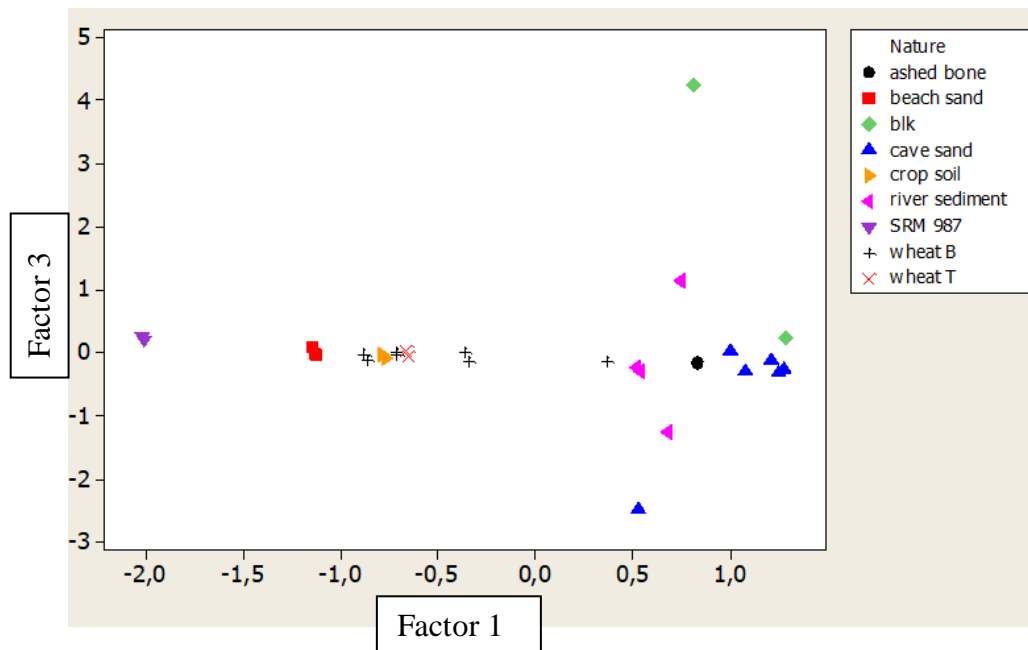


**Figure 25.** Dispersion graph between Factor 1 and Factor 3.

#### 4.3.4. Classification of samples depending on their origin or nature

Classification of the samples in clusters depending on their origin (Name) or nature was done by the HCA option in STATGRAPHICS. Since it is performed with Euclidean distances, the smaller the distance value the better, since it would signify that they are more closely related.

The separation is quite satisfactory (**Figure 26**). The samples from the north of Spain are in one cluster and the ones from the south in another. Most of the samples of the same nature are together in sub clusters, with little Euclidean distance between them, which demonstrates their similarity. C-NIST8704 and C-LM 21154-04 are quite far away from their counterparts, although it can be due to the fact that the amount of samples is very small and needs increasing.

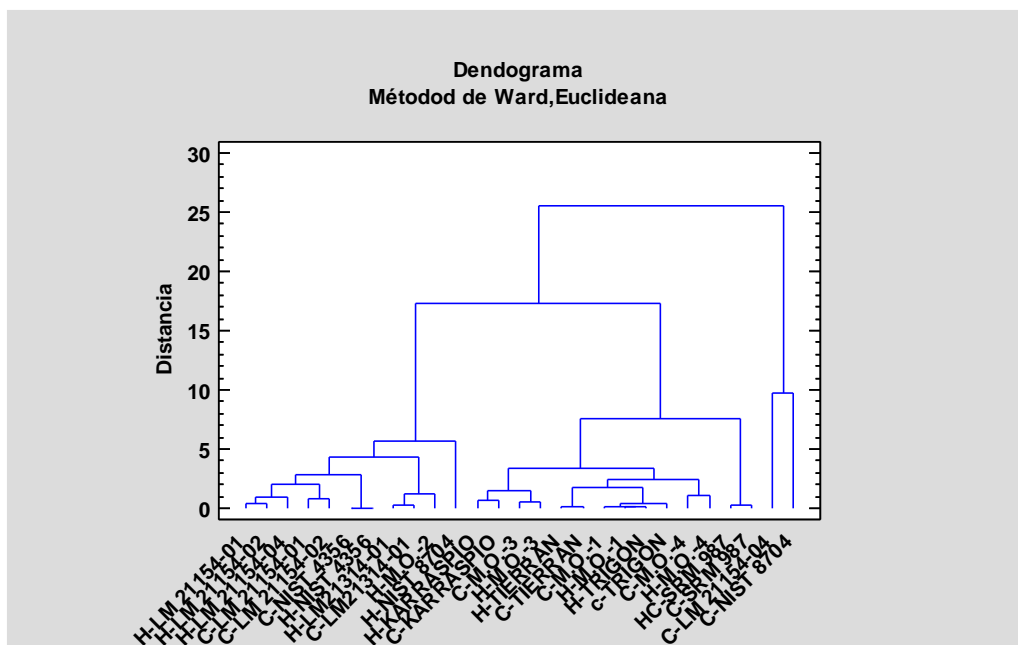


**Figure 26.** Dendrogram of the samples, sorted by their origin. The prefix C indicates the commercial cartridge and the prefix H indicates the handmade cartridge.

The results above are confirmed in **Figure 27**. Similar natured samples are clustered together, taking into account their origin. This could be expanded once more samples are available for analysis.

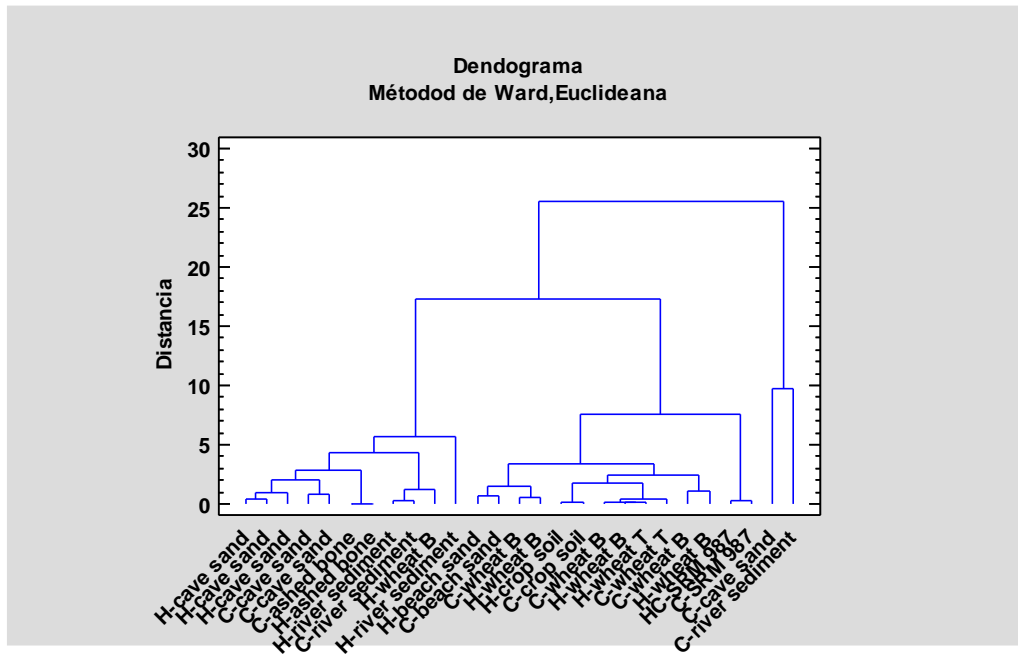


**Figure 27.** Dendrogram of the samples, sorted by their Nature. The prefix C indicates the commercial cartridge and the prefix H indicates the handmade cartridge.

For the variables a HCA was performed, and the Dendrogram was obtained (**Figure 28**). As expected, isotopic variations are the most correlated ones, confirming the Pearson coefficient results on **Figure 22**.

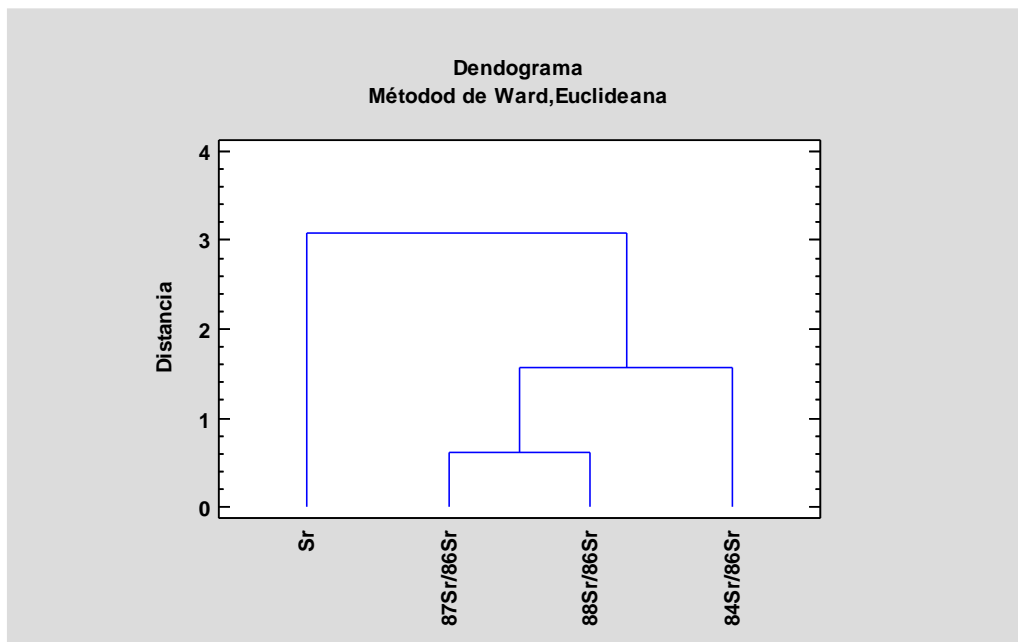


**Figure 28.** Dendrogram of the variables.

The results obtained via PCA and FA were confirmed with the HCA. There is trend among all samples: those with a similar nature tend to cluster together, either when studying elemental Sr or isotopes ratio. The samples are, at the same time, clustered together depending on their origin.

Overall, the statistical work conducted in this study yields satisfactory preliminary results. This is intended for the construction of a pattern recognition model for strontium isotope mapping. However, there are slight inconsistencies of the model detailed above; this can be due to the limited sampling number. The ultimate goal of this research is to analyse a vast amount of samples, soil and plant ones, with this model, which will greatly reduce the error and will, in its stead, enhance the precision and accuracy of this technique.

## 5. Conclusions

1. Two methods for ion chromatography were tested, yielding similar results from a statistical point of view. Although the hand-made cartridges exhibited less variation on the results, commercial cartridges were much faster with similar results. This confirms the possibility to use commercial cartridges when a vast amount of sample analysis is required, while using hand-made columns for more complicated ones, with the security of knowing both methods are comparable between each other.
2. It was determined that the strontium concentration and  $^{87}\text{Sr}/^{86}\text{Sr}$  ratio were the most important variables when determining the origin and nature of a sample. Both of them are important, to accurately assess the samples' origin.
3. The statistical framework was successfully developed, using the amount of samples analyzed to start feeding the pattern recognition model. It proved the possibility to accurately differentiate between not only the origins of the samples, but between the nature of them.

The developed framework for sample preparation and statistical pattern recognition model is a success. It allows reducing the time used in sample preparation, while making sure the results are not greatly compromised, as well as determining the origin and nature of a sample with minimal testing. Specially in a field like geochronology and paleoresearch, where sometimes certain samples can be scarce with tiny amounts of them available for analysis, this model provides the most information.

Limitations of this study can be solved increasing the amount of samples tested, improving the pattern recognition model and decreasing the variance between samples.

It can also be the starting point of a longer research focused on the mapping of strontium across the Iberian Peninsula, as well as more detailed studies of the strontium cycle across different lithology.

## 6. References

- [1] Valera, A. C., Žalaitė, I., Maurer, A. F., Grimes, V., Silva, A. M., Ribeiro, S., ... & Dias, C. B. (2020). Addressing human mobility in Iberian Neolithic and Chalcolithic ditched enclosures: The case of Perdigões (South Portugal). *Journal of Archaeological Science: Reports*, 30, 102264.
- [2] Fernández-Crespo, T., Le Roux, P. J., Ordoño, J., Ditchfield, P. W., & Schulting, R. J. (2020). The life-history of a late Mesolithic woman in Iberia: A sequential multi-isotope approach. *Quaternary International*, 566, 233-244.
- [3] Ericson, J.E. (1985) Strontium isotope characterization in the study of prehistoric human ecology. *Journal of Human Evolution*, 14(5), 503-514.
- [4] Peters, K.E., Walters, C.C. and Moldovan, J.M., (2007). The biomarker guide: Volume 1, Biomarkers and isotopes in the environment and human history. *Cambridge university press*.
- [5] Cheesman, A.W., Cernusak L. A. (2016) Isoscapes: a new dimension in community ecology. *Tree Physiology*, 36(12), 1, 1456–1459.
- [6] Semenishchev, V.S., Voronina, A.V. (2020). Isotopes of Strontium: Properties and Applications. In: Pathak, P., Gupta, D. (eds) *Strontium Contamination in the Environment. The Handbook of Environmental Chemistry*, vol 88. Springer, Cham.
- [7] Wang, J., Di, Y., Asael, D., Planavsky, N. J., & Tarhan, L. G. (2023). An investigation of factors affecting high-precision Sr isotope analyses ( $^{87}\text{Sr}/^{86}\text{Sr}$  and  $\delta^{88}\text{Sr}/^{86}\text{Sr}$ ) by MC-ICP-MS. *Chemical Geology*, 621, 121365.
- [8] Maurer, A. F., Galer, S. J., Knipper, C., Beierlein, L., Nunn, E. V., Peters, D., ... & Schöne, B. R. (2012). Bioavailable  $^{87}\text{Sr}/^{86}\text{Sr}$  in different environmental samples—Effects of anthropogenic contamination and implications for isoscapes in past migration studies. *Science of the Total Environment*, 433, 216-229.

- [9] *IUPAC Compendium of Chemical Terminology*, 3rd ed. International Union of Pure and Applied Chemistry; 2006. Online version 3.0.1, 2019.
- [10] Bentley, R.A. (2006) Strontium Isotopes from the Earth to the Archaeological Skeleton: A Review. *Journal of Archaeological Method and Theory*, 13(3).
- [11] Scrimgeour, C. M., & Robinson, D. (2003). Stable isotope analysis and applications. In *Soil and environmental analysis* ( 348-393). CRC Press.
- [12] Banner, J. L. (2004). Radiogenic isotopes: systematics and applications to earth surface processes and chemical stratigraphy. *Earth-Science Reviews*, 65(3-4), 141-194.
- [13] Schwarcz, H. P., White, C. D., & Longstaffe, F. J. (2010). Stable and radiogenic isotopes in biological archaeology: some applications. *Isoscapes: Understanding movement, pattern, and process on Earth through isotope mapping*, 335-356.
- [14] Coldwell, B.C., Pérez, N.M., Vaca, M.C., Pankhurst, M.J., Hernández, P.A., Rodriguez, G.V.M., Padrón, E., Asensio-Ramos, M., Ribeiro, S., Santos, J.F. (2022) Strontium Isotope Systematics of Tenerife Wines (Canary Islands): Tracing Provenance in Ocean Island Terroir. *Beverages* , 8 (9).
- [15] Capo, R.C., Stewart, B.W. and Chadwick, O.A., (1998). Strontium isotopes as tracers of ecosystem processes: theory and methods. *Geoderma*, 82(1-3), 197-225.
- [16] Cavazzini, G., Roccatò, D., & Fasson, A. (2022) The determination of the isotopic composition of strontium. *International Journal of Mass Spectrometry*, 471.
- [17] Blum, J. D., Erel, Y. & Brown, K. (1993)  $^{87}\text{Sr}/^{86}\text{Sr}$  ratios of Sierra Nevada stream waters: implications for relative mineral weathering rates. *Geochimica et Cosmochimica Acta*, 58, 5019-5025.

- [18] Nigro, A., Sappa, G., & Barbieri, M. (2017). Strontium isotope as tracers of groundwater contamination. *Procedia Earth and Planetary Science*, 17, 352-355.
- [19] Wu, Y. S., Zhou, K. F., Li, N., & Chen, Y. J. (2017). Zircon U–Pb dating and Sr–Nd–Pb–Hf isotopes of the ore-associated porphyry at the giant Donggebi Mo deposit, Eastern Tianshan, NW China. *Ore Geology Reviews*, 81, 794-807.
- [20] Duller, G. A. T. (2000). Dating methods: geochronology and landscape evolution. *Progress in Physical Geography: Earth and Environment*, 24(1), 111-116.
- [21] Åberg, G. (1995). The use of natural strontium isotopes as tracers in environmental studies. *Water, Air, and Soil Pollution*, 79, 309-322..
- [22] McNutt, R. H. (2000). Strontium isotopes. In *Environmental tracers in subsurface hydrology* ( 233-260). Boston, MA: Springer US.
- [23] Prohaska, T., Irrgeher, J., Benefield, J. , Böhlke, J. K. , Chesson, L. A., Coplen, T. B., Ding, T., Dunn, P. J. H. , Gröning, M. , Holden, N. E. , Meijer, H. A. J., Moossen, H., Possolo, A., Takahashi, Y., Vogl, J., Walczyk, T., Wang, J., Wieser, M. E., Yoneda, S., Meija, J. (2022) Standard atomic weights of the elements 2021. *Pure and Applied Chemistry, IUPAC Technical Report.*, 94(5), 573-600.
- [24] Nedobukh, T. A., & Semenishchev, V. S. Strontium: source, occurrence, properties, and detection. In *Handbook of Environmental Chemistry.*, 2020, 88, 1-23. Springer Verlag.
- [25] Nielsen, E., Greve, K., Ladefoged, O. (2013) Strontium, inorganic and soluble salts. Evaluation of health hazards and proposal of health based quality criteria for drinking water. Danish Ministry of the Environment, Environmental protection agency. Environmental project No.1525, 2013.
- [26] Hajj, F., Poszwa, Anne., Bouchez, J., Guerold, F. (2017) Radiogenic and “stable” strontium isotopes in provenance studies: A review and first results on archeological wood from shipwrecks. *Journal of Archaeological Science*, 86, 24-49.

- [27] Aguzzoni, A., Bassi, M., Robatscher, P., Scandellari, F., Tirler, W., Tagliavini, M. (2019) Intra- and Intertree Variability of the  $^{87}\text{Sr}/^{86}\text{Sr}$  Ratio in Apple Orchards and Its Correlation with the Soil  $^{87}\text{Sr}/^{86}\text{Sr}$  Ratio. *Journal of Agricultural and Food Chemistry*, 67 (20), pp 5728-5735.
- [28] Černý, P., Chapman, R., Teertstra, D., Novák, M. (2003). Rubidium- and cesium-dominant micas in granitic pegmatites. *American Mineralogist*. 88, 1832-1835.
- [29] Rosman, K.J.R., Taylor, P.D.P. (1998) Isotopic compositions of the elements 1997. *Pure and applied chemistry*, 70, pp-217-236.
- [30] Gargi, S.P. (2019) Measuring the decay constant of  $^{87}\text{Rb}$ : Is the decay in radioisotopes linear? Manifestation and disintegration of the matter in space-time, and age of the Universe. *Solid Earth Sciences*, 4 (1), 12-26.
- [31] Scher, H. D., E. M. Griffith, and W. P. Buckley (2014), Accuracy and precision of  $^{88}\text{Sr}/^{86}\text{Sr}$  and  $^{87}\text{Sr}/^{86}\text{Sr}$  measurements by MC-ICPMS compromised by high barium concentrations, *Geochem. Geophys. Geosyst.*, 15, 499–508,
- [32] Bohm, F., A. Eisenhauer, J. W. Tang, M. Dietzel, A. Krabbenhoft, B. Kisakurek, and C. Horn (2012), Strontium isotope fractionation of planktic foraminifera and inorganic calcite, *Geochim. Cosmochim. Acta*, 93, 300–314.
- [33] Peucker-Ehrenbrink, B., & Fiske, G. J. (2019). A continental perspective of the seawater  $^{87}\text{Sr}/^{86}\text{Sr}$  record: A review. *Chemical Geology*, 510, 140-165.
- [34] Peucker-Ehrenbrink, B., & Fiske, G. J. (2019). A continental perspective of the seawater  $^{87}\text{Sr}/^{86}\text{Sr}$  record: A review. *Chemical Geology*, 510, 140-165.
- [35] Birck, J., Allegre, (1979). C.  $^{87}\text{Rb}$ - $^{87}\text{Sr}$  chronology of the Binda howardite. *Nature* 282, 288–289.

- [36] Minster, JF., Birck, JL. & Allègre, C. (1982). Absolute age of formation of chondrites studied by the  $^{87}\text{Rb}$ - $^{87}\text{Sr}$  method. *Nature* 300, 414–419
- [37] Scott Anderson F., Levine J., and Whitaker T. (2014) Dating the Martian meteorite Zagami by the  $^{87}\text{Rb}$ - $^{87}\text{Sr}$  isochron method with a prototype *in situ* resonance ionization mass spectrometer, *Rapid Commun. Mass Spectrom.*, 29, 191–204.
- [38] Snelling, A. A. 2003. The Relevance of Rb-Sr, Sm-Nd, and Pb-Pb Isotope Systematics to Elucidation of the Genesis and History of Recent Andesite Flows at Mt. Ngauruhoe, New Zealand, and the Implications for Radioisotopic Dating. *Proceedings of the Fifth International Conference on Creationism*. R. L. Ivey, Jr., ed. Pittsburgh, PA: Creation Science Fellowship, 285-303.
- [39] P. C. Smalley, A. C. Higgins, R. J. Howarth, H. Nicholson, C. E. Jones, N.H.M. Swinburne, J. Bessa. (1994) Seawater Sr isotope variations through time: A procedure for constructing a reference curve to date and correlate marine sedimentary rocks. *Geology*, 22 (5), 431–434.
- [40] Åberg, G., Jacks, G., Hamilton, P.J. (1989) Weathering rates and  $^{87}\text{Sr}/^{86}\text{Sr}$  ratios: An isotopic approach. *Journal of Hydrology*, 109( 1–2), 65-78.
- [41] Willmes, M. (2015). Strontium isotope tracing of prehistoric human mobility in France.
- [42] Vanhaecke, F., & Degryse, P. (Eds.). (2012). *Isotopic analysis: fundamentals and applications using ICP-MS*. John Wiley & Sons.
- [43] Becker, J.S., Dietze, H. J. (2000). Precise and accurate isotope ratio measurements by ICP-MS. *Fresenius' journal of analytical chemistry*, 368, 23-30.
- [44] Vanhaecke, F., Balcaen, L., & Taylor, P. (1999). Use of ICP-MS for isotope ratio measurements. *Inductively coupled plasma spectrometry and its applications*, 160.

- [45] Hodell, D. A., Quinn, R. L., Brenner, M., & Kamenov, G. (2004). Spatial variation of strontium isotopes ( $^{87}\text{Sr}/^{86}\text{Sr}$ ) in the Maya region: a tool for tracking ancient human migration. *Journal of Archaeological science*, *31*(5), 585-601.
- [46] Cuello-del Pozo, P. (2019) Análisis preliminar de los isótopos estables del estroncio ( $^{87}\text{Sr}/^{86}\text{Sr}$ ) biodisponibles en la isla de Lanzarote: Propuesta para la creación de una base de datos de referencia para su aplicación en la arqueología canaria. *Anuario de Estudios Atlánticos, AEA*, *65*, 1-17.
- [47] Willmes, M., McMorrow, L., Kinsley, L., Armstrong, R., Aubert, M., Eggins, S., ... & Grün, R. (2014). The IRHUM (Isotopic Reconstruction of Human Migration) database—bioavailable strontium isotope ratios for geochemical fingerprinting in France. *Earth System Science Data*, *6*(1), 117-122.
- [48] Bataille, C. P., von Holstein, I. C., Laffoon, J. E., Willmes, M., Liu, X. M., & Davies, G. R. (2018). A bioavailable strontium isoscape for Western Europe: A machine learning approach. *PloS one*, *13*(5), e0197386.
- [49] Bataille, C. P., Crowley, B. E., Wooller, M. J., & Bowen, G. J. (2020). Advances in global bioavailable strontium isoscapes. *Palaeogeography, Palaeoclimatology, Palaeoecology*, *555*, 109849.
- [50] Kootker, L. M., van Lanen, R. J., Kars, H., & Davies, G. R. (2016). Strontium isoscapes in The Netherlands. Spatial variations in  $^{87}\text{Sr}/^{86}\text{Sr}$  as a proxy for palaeomobility. *Journal of Archaeological Science: Reports*, *6*, 1-13.
- [51] Lugli, F., Cipriani, A., Bruno, L., Ronchetti, F., Cavazzuti, C., & Benazzi, S. (2022). A strontium isoscape of Italy for provenance studies. *Chemical Geology*, *587*, 120624.
- [52] James, H. F., Adams, S., Willmes, M., Mathison, K., Ulrichsen, A., Wood, R., ... & Grün, R. (2022). A large-scale environmental strontium isotope baseline map of Portugal for archaeological and paleoecological provenance studies. *Journal of Archaeological Science*, *142*, 105595.

- [53] Linscott, B., Pike, A. W., Angelucci, D. E., Cooper, M. J., Milton, J. S., Matias, H., & Zilhão, J. (2023). Reconstructing Middle and Upper Paleolithic human mobility in Portuguese Estremadura through laser ablation strontium isotope analysis. *Proceedings of the National Academy of Sciences*, *120*(20), e2204501120.
- [54] Díaz-del-Río, P., Uriarte, A., Becerra, P., Pérez-Villa, A., Vicent, J. M., & Díaz-Zorita, M. (2022). Paleomobility in Iberia: 12 years of strontium isotope research. *Journal of Archaeological Science: Reports*, *46*, 103653.
- [55] Xu, C., Wang, J., & Chen, J. (2012). Solvent Extraction of Strontium and Cesium: A Review of Recent Progress. *Solvent Extraction and Ion Exchange*, *30*(6), 623–650.
- [56] Becker, J. S. (2005). Recent developments in isotope analysis by advanced mass spectrometric techniques Plenary lecture. *Journal of Analytical Atomic Spectrometry*, *20*(11), 1173-1184.
- [57] Bellefroid, E. J., Planavsky, N. J., Miller, N. R., Brand, U., & Wang, C. (2018). Case studies on the utility of sequential carbonate leaching for radiogenic strontium isotope analysis. *Chemical Geology*, *497*, 88-99.
- [58] Bayon, G., German, C. R., Boella, R. M., Milton, J. A., Taylor, R. N., & Nesbitt, R. W. (2002). An improved method for extracting marine sediment fractions and its application to Sr and Nd isotopic analysis. *Chemical Geology*, *187*(3-4), 179-199.
- [59] Laffoon, J. E., Davies, G. R., Hoogland, M. L., & Hofman, C. L. (2012). Spatial variation of biologically available strontium isotopes ( $^{87}\text{Sr}/^{86}\text{Sr}$ ) in an archipelagic setting: a case study from the Caribbean. *Journal of Archaeological Science*, *39*(7), 2371-2384.
- [60] Rodriguez, M., Suarez, J. A., & Espartero, A. G. (1996). Separation of radioactive strontium by extraction using chromatographic resin. *Nuclear Instruments and Methods in Physics Research Section A: Accelerators, Spectrometers, Detectors and Associated Equipment*, *369*(2-3), 348-352.

- [61] Yang, Y. H., Wu, F. Y., Liu, Z. C., Chu, Z. Y., Xie, L. W., & Yang, J. H. (2012). Evaluation of Sr chemical purification technique for natural geological samples using common cation-exchange and Sr-specific extraction chromatographic resin prior to MC-ICP-MS or TIMS measurement. *Journal of Analytical Atomic Spectrometry*, 27(3), 516-522.
- [62] Wassenburg, J. A., Riechelmann, S., Schröder-Ritzrau, A., Riechelmann, D. F., Richter, D. K., Immenhauser, A., ... & Scholz, D. (2020). Calcite Mg and Sr partition coefficients in cave environments: Implications for interpreting prior calcite precipitation in speleothems. *Geochimica et Cosmochimica Acta*, 269, 581-596.
- [63] Dasch, E. J. (1969). Strontium isotopes in weathering profiles, deep-sea sediments, and sedimentary rocks. *Geochimica et Cosmochimica Acta*, 33(12), 1521-1552.
- [64] Alonzi, E., Pacheco-Forés, S. I., Gordon, G. W., Kuijt, I., & Knudson, K. J. (2020). New understandings of the sea spray effect and its impact on bioavailable radiogenic strontium isotope ratios in coastal environments. *Journal of Archaeological Science: Reports*, 33, 102462.
- [65] Duckworth, R. B., & Hawthorn, J. (1960). Uptake and distribution of strontium in vegetables and cereals. *Journal of the Science of Food and Agriculture*, 11(4), 218-225.

## Lista de Figuras

**Figure 1.** Strontium cycle and its influences.

**Figure 2.** Range of variation of  $^{87}\text{Sr}/^{86}\text{Sr}$  ratios (values in italic) and  $\delta^{88}\text{Sr}/^{86}\text{Sr}$  (‰) values in rocks, atmospheric dust and different water compartments at global scale

**Figure 3.** Work flow of the steps followed in the laboratory work. The one on the left is the work flow for isotopic analysis, and the one on the right is the one for concentration analysis.

**Figure 4.** Map of Iberian Peninsula Spain. The red circles indicate the origins of the samples

**Figure 5.** Grains of wheat taken from Burgos (Spain)

**Figure 6.** Wheat seeds from Tudela (Navarra, Spain)

**Figure 7.** Soil samples. From left to right, top to bottom: LM 21154-01, LM21154-02, LM21154-04, KARRASPIO, LM21312-01, TIERRAN.

**Figure 8.** Cut up sections of the wheat stem.

**Figure 9.** From left to right, whole seed, bare seeds and chaffs.

**Figure 10.** Oven at CENIEH laboratory

**Figure 11.** ultraWave Single reaction chamber microwave digestion at CENIEH laboratory

**Figure 12.** Close up of micro column

**Figure 13.** General setup of commercial columns

**Figure 14.** ICP-OES at CENIEH.

**Figure 15.** HR-ICP-MS, ELEMENT XR at CENIEH.

**Figure 16.** MC-ICP-MS, NEPTUNE at CENIEH.

**Figure 17.** Graphical representation of the SRM987  $^{87}\text{Sr}/^{86}\text{Sr}$  ratio experimental measurements along with the literature values.

**Figure 18.** Comparison between cave sands'  $^{87}\text{Sr}/^{86}\text{Sr}$  ratios from hand-made and commercial cartridges for the samples (From left to right, each pair of dots: LM 21154-01, LM21154-02, LM 21154-04)

**Figure 19.** Comparison between beach sand, river sediment, crop soil and NIST 8704  $^{87}\text{Sr}/^{86}\text{Sr}$  ratios from hand-made and commercial cartridges for the samples (From left to right, each pair of dots: KARRASPIO, LM 21314-01, TIERRAN, NIST 8704)

**Figure 20.** Comparison between Burgos wheat  $^{87}\text{Sr}/^{86}\text{Sr}$  ratios from hand-made and commercial cartridges for the samples (From left to right, each pair of dots: M.O.-1, M.O.-2, M.O.-3, M.O.-4)

**Figure 21.** Comparison between Tudela wheat and NIST 4356  $^{87}\text{Sr}/^{86}\text{Sr}$  ratios from hand-made and commercial cartridges for the samples (From left to right, each pair of dots: TRIGON, NIST 4356)

**Figure 22.** Pearson correlation coefficients matrix for the different variables

**Figure 23.** PCA sedimentation graph.

**Figure 24.** Dispersion graph between Factor 1 and Factor 2.

**Figure 25.** Dispersion graph between Factor 1 and Factor 3.

**Figure 26.** Dendrogram of the samples, sorted by their origin. The prefix C indicates the commercial cartridge and the prefix H indicates the handmade cartridge.

**Figure 27.** Dendrogram of the samples, sorted by their Nature. The prefix C indicates the commercial cartridge and the prefix H indicates the handmade cartridge

**Figure 28.** Dendrogram of the variables.

## Lista de Tablas

**Table 1.** Strontium concentration on different nature samples

**Table 2.** Summary of the samples used in this study

**Table 3.** Expected values of  $^{87}\text{Sr}/^{86}\text{Sr}$  ratio for SRM987

**Table 4.** Measure parameters of ICP-OES

**Table 5.** Measure parameters of HR-ICP-MS, ELEMENT XR.

**Table 6.** Measure parameters of MC-ICP-MS, NEPTUNE

**Table 7.** Total digestion Sr concentration results in ICP-OES and SF-ICP-MS

**Table 9.** Sr leachate concentration results in ICP-OES and SF-ICP-MS

**Table 10.**  $^{87}\text{Sr}/^{86}\text{Sr}$  ratio results for SRM 987.

**Table 11.**  $^{88}\text{Sr}/^{86}\text{Sr}$  and  $^{84}\text{Sr}/^{86}\text{Sr}$  ratios of the samples

**Table 12.**  $^{88}\text{Sr}/^{86}\text{Sr}$  and  $^{84}\text{Sr}/^{86}\text{Sr}$  ratios for samples

**Table 13.** KS test resulting values for each variable

**Table 14.** P-values for the correlation matrix.

**Table 15.** Values for the principal components.

**Table 16.** Weight of each component for the variables.

**Table 17.** Loadings of principal components.

**Table 18.** Loadings of FA without rotation.

**Table 19.** Scores of each one of the samples

**Table 20.** Loadings before rotating

**Table 21.** Loadings after varimax rotation.

**Table 22.** Scores for the samples with Varimax rotation